Localization of a Surgical Tool Inside Biological Tissue Using 3D Ultrasound Images

Martin Barva, Jan Kybic, Václav Hlaváč
Center for Machine Perception, Czech Technical University in Prague, Czech Republic
Jean-Martial Mari, Hervé Liebgott, Christian Cachard
CREATIS, Institut National des Sciences Appliqées de Lyon, France

PRESENTATION OUTLINE

- Motivation
- Problem definition
- Description of proposed methods
  - Two methods for axis object localization.
  - Tip localization.
- Results
- Conclusions

MOTIVATION

- Small instruments are often introduced into the body:
  - Needle aspiration biopsy.
  - Prostate brachytherapy.
  - Laparoscopic surgery.
  - ⇒ Neuronal cortical recording.
- Tracking of needle/electrode inside biological tissue is important to:
  - Place the instrument into a specific tissue region.
  - Avoid important organ structures (blood-vessels).
  - Compensate for organ movement.

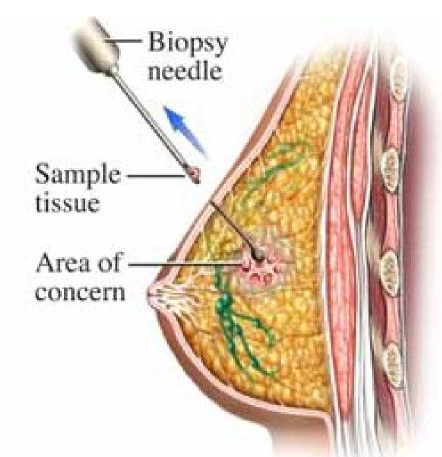

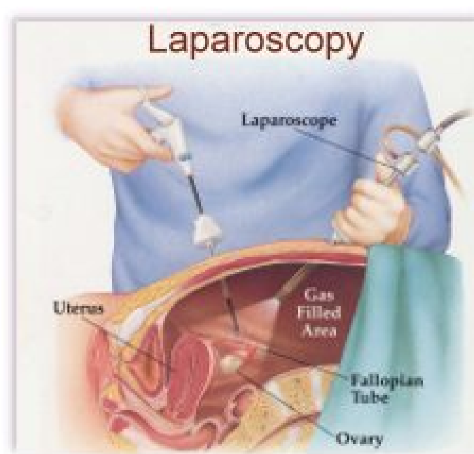

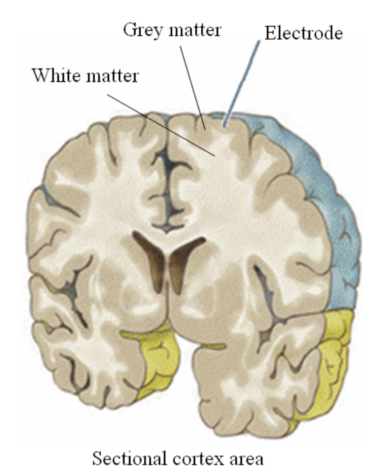

COMMON TECHNIQUES FOR TOOL LOCALIZATION

- Stereotaxy – rigid frames. Accurate ≈ 0.1 mm, movement restriction.
- Frameless localization – RF coils, optical tracking. Accuracy ≈ 5 mm.

⇒ Image guidance – CT, MRI, US.

- Advantages of ultrasound:
  - Real-time, no ionizing radiation.
  - Compatible with metallic surgical instruments.
  - Scanning device is portable, easy to manipulate, and relatively cheap.

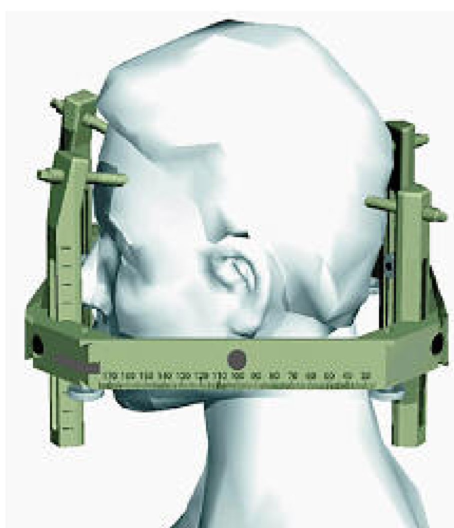

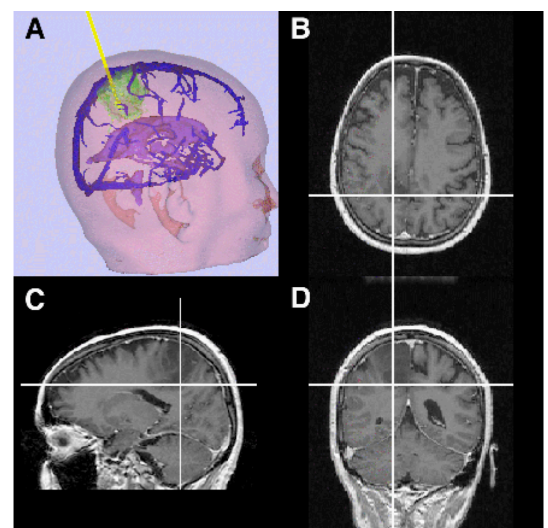

PROBLEM DESCRIPTION

- 3D US scan of ROI.
- Task: determine electrode position. Additionally, estimate localization accuracy.
- Difficulties:
  - Speckle noise.
  - Signal loss due to total reflection ⇒ electrode appears irregular and incomplete.
  - Electrode shape changes with position and orientation.
  - Large data sets.

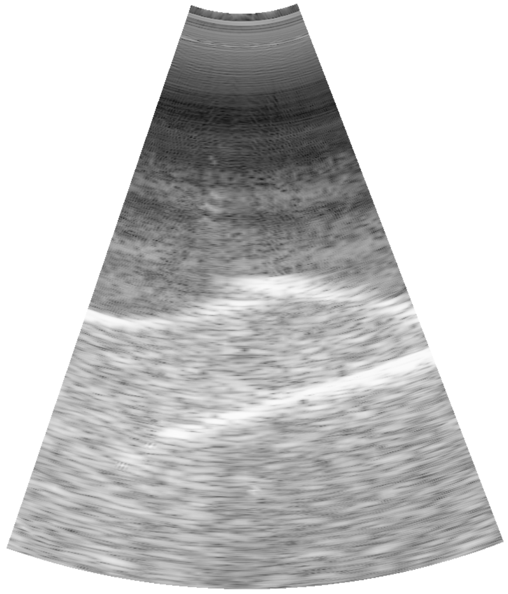

METHODS

- Assumptions:
  - Region of voxels with higher intensity.
  - Approximately cylindrical shape with curvilinear axis.
- Two subtasks:
  - Localization of electrode axis. Two algorithms proposed:
    - Method I – Parallel Integral Projection Transform.
    - Method II – RANSAC-based model fitting.
  - Electrode tip localization.

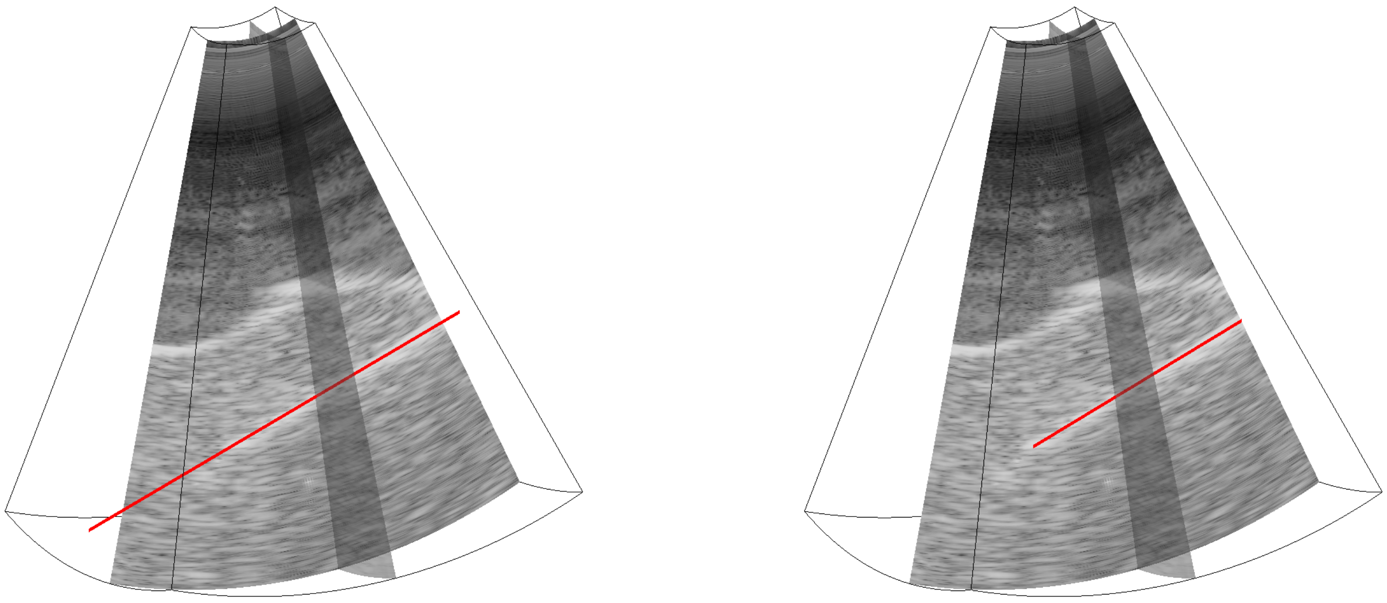

Axis localization
Method I – Parallel Integral Projection Transform

METHOD I – PIP TRANSFORM

- 3D image function $I : A \rightarrow B$, with $A \subset \mathbb{N}^3$, $B \subset \mathbb{R}_0^+$.
- Formalization by Parallel Integral Projection (PIP) transform:

$$\mathcal{P}_I(u, v, \alpha, \beta) = \int_{-\infty}^{\infty} I\left(\mathbf{R}(\alpha, \beta) \cdot (u, v, \tau)^T\right) \mathrm{d}\tau,$$

  where $\mathbf{R}(\alpha, \beta)$ is 3D rotation matrix.
- Integral of function I along a line defined by vector $\vec{w} = \mathbf{R}(\alpha, \beta) \cdot (0, 0, 1)^T$ and point $Q = \mathbf{R}(\alpha, \beta) \cdot (u, v, 0)^T$.
- $\mathcal{P}_I(u, v, \alpha, \beta)$ is periodic along α, β with π.
- Similarity to 3D Radon Transform.

METHOD I – AXIS LOCALIZATION WITH PIP

- PIP is maximized when image is projected along electrode axis.
- Localization of electrode axis $\Rightarrow$ maximization of the PIP.
- If $\mathcal{P}_I$ is maximized at $(u_{max}, v_{max}, \alpha_{max}, \beta_{max})$, then electrode axis is given by

$$a(t) = \mathbf{R}(\alpha_{max}, \beta_{max}) \cdot (u_{max}, v_{max}, t)^T; \qquad \forall t \in \mathbb{R}.$$

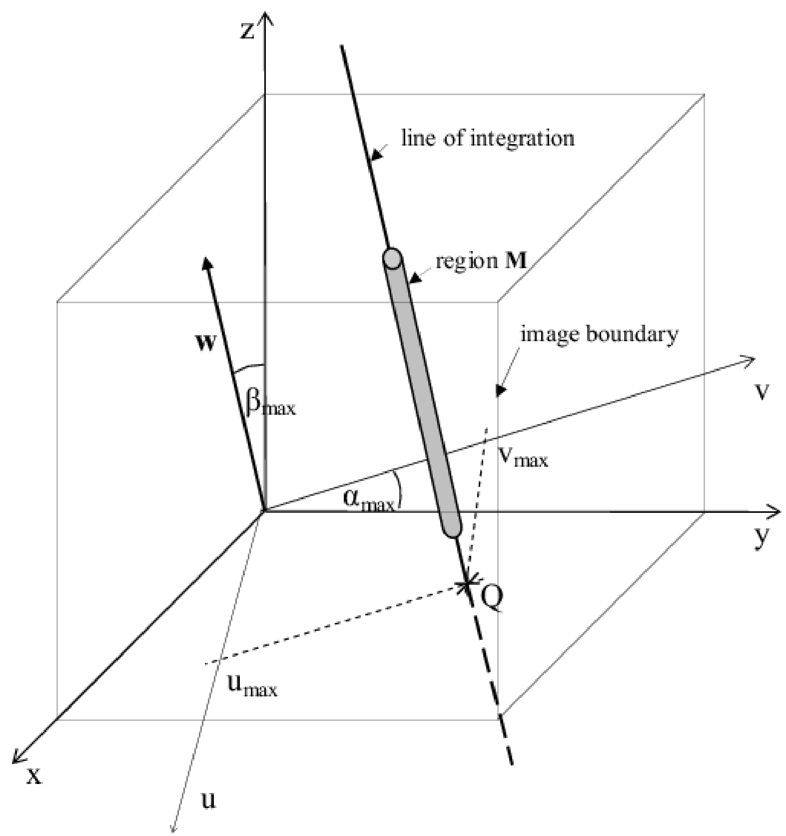

METHOD I – MAXIMIZATION OF PIP

- Discrete grid with steps $\Delta_u, \Delta_v, \Delta_\alpha, \Delta_\beta$.
- Maximization of $\mathcal{P}_I$ is decomposed:
  - Inner loop: Maximize for u, v (exhaustive search),

$$J(\alpha_k, \beta_l) = \max_{u_i, v_j} \mathcal{P}_I(u_i, v_j, \alpha_k, \beta_l),$$

  - Outer loop: Maximize for α, β,

$$\arg\max_{\alpha_k, \beta_l} J(\alpha_k, \beta_l) = \arg \max_{u_i, v_j, \alpha_k, \beta_l} \mathcal{P}_I(u_i, v_j, \alpha_k, \beta_l).$$

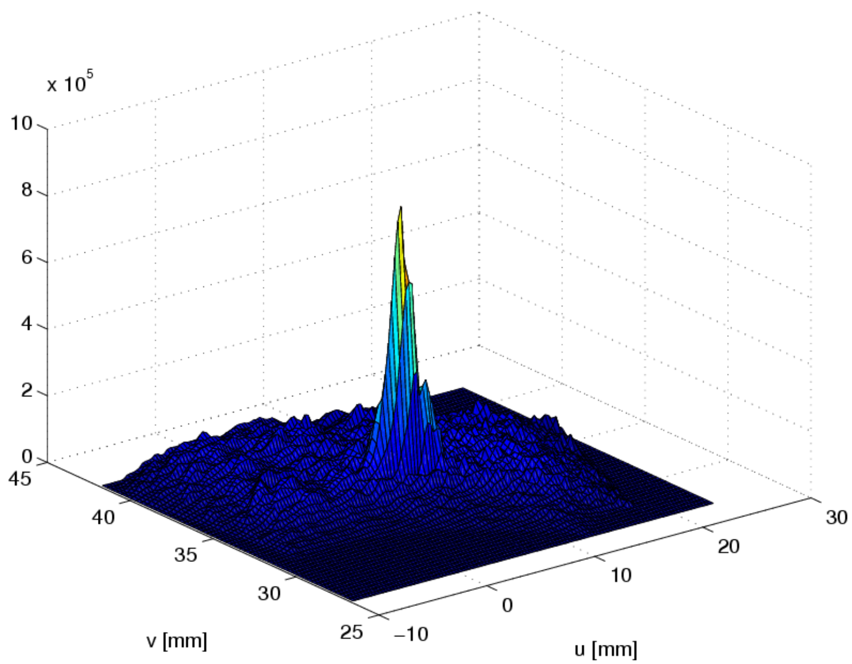

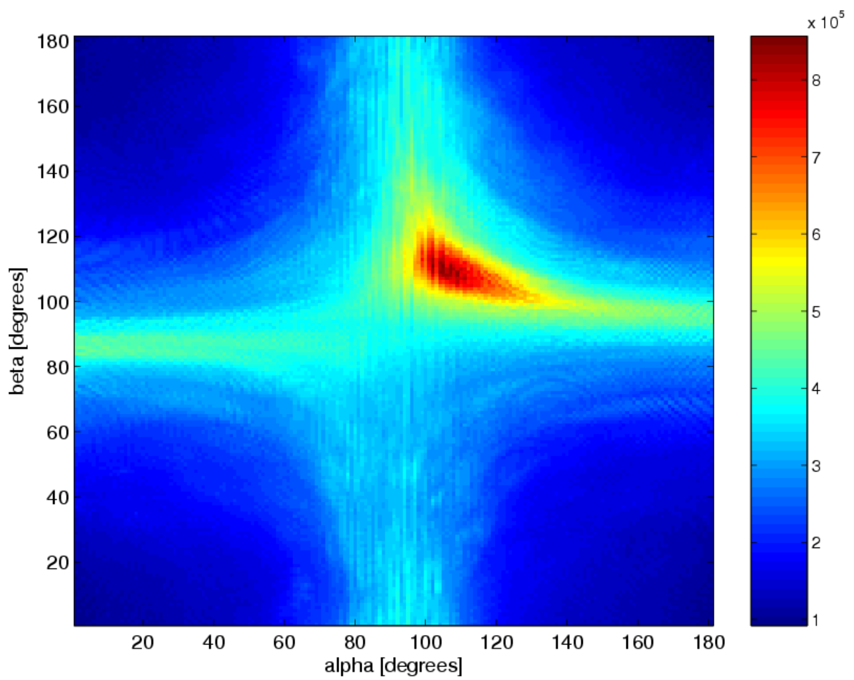

METHOD I – HIERARCHICAL MESH-GRID SEARCH

- Hierarchical maximization of $J(\alpha_k, \beta_l)$.

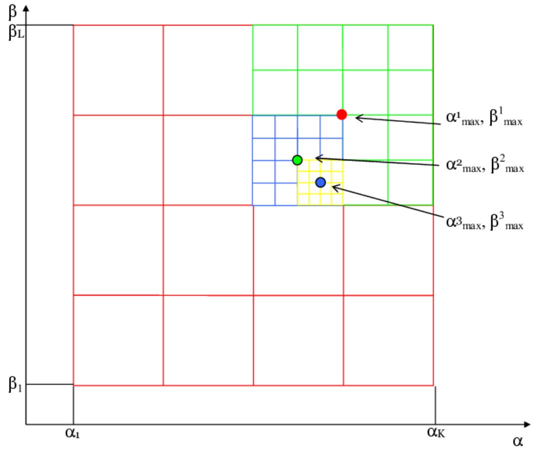

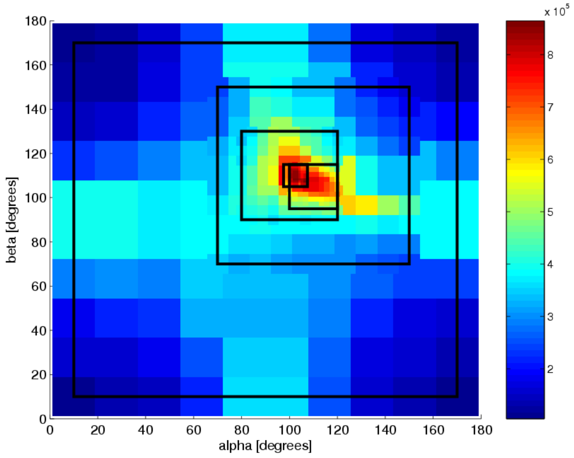

Axis localization
Method II – RANSAC-based model fitting

METHOD II – PRE-PROCESSING

- 3D image function $I : A \rightarrow B$, with $A \subset \mathbb{N}^3$, $B \subset \mathbb{R}_0^+$.
- Threshold T: set A_e (electrode), A_b (background).
- Gamma pdf models intensity of voxels in A,

$$P_\Gamma(I; k, \varphi) = I^{(k-1)} \frac{e^{-I/\varphi}}{\varphi^k \Gamma(k)}$$

- Parameters (k, φ) are ML estimates from training data.
- Threshold T is set as 95% quantile of Gamma cdf.

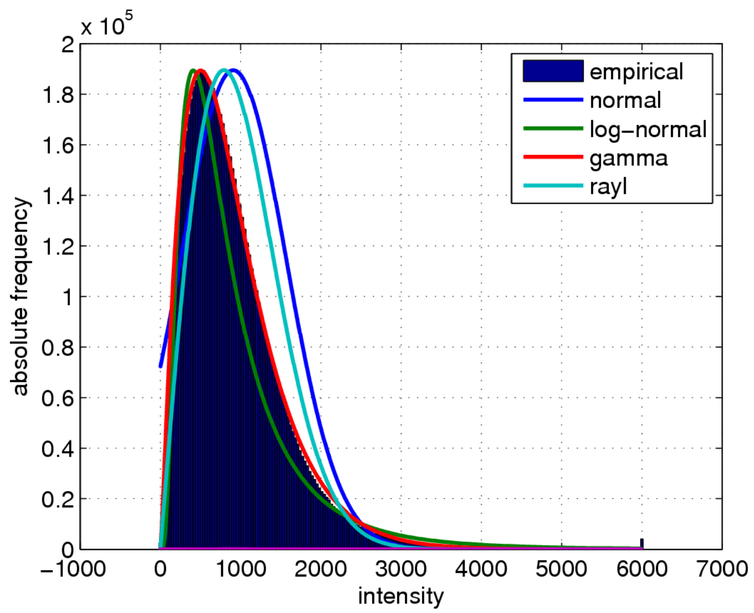

METHOD II – ELECTRODE AXIS MODEL

- Axis is approximated by cubic polynomial $a(t;\theta)$

$$\begin{aligned} x(t) &= a_0 + a_1 t + a_2 t^2 + a_3 t^3 \\ y(t) &= b_0 + b_1 t + b_2 t^2 + b_3 t^3 \\ z(t) &= c_0 + c_1 t + c_2 t^2 + c_3 t^3,\ t \in \mathbb{R}, \end{aligned}$$

with parameter vector $\theta = (a_0, a_1, a_2, a_3, b_0, b_1, b_2, b_3, c_0, c_1, c_2, c_3)$.

- Degree of polynomial chosen as trade-off between flexibility and oscillations.

MODEL II – ELECTRODE INTENSITY MODEL

- Estimate of conditional pdf $P(I \mid r)$ for voxels close to axis.
- For various voxel-to-axis distances r, histogram of voxel intensity I.
- Bin size was set according to Freedman-Diaconis rule.

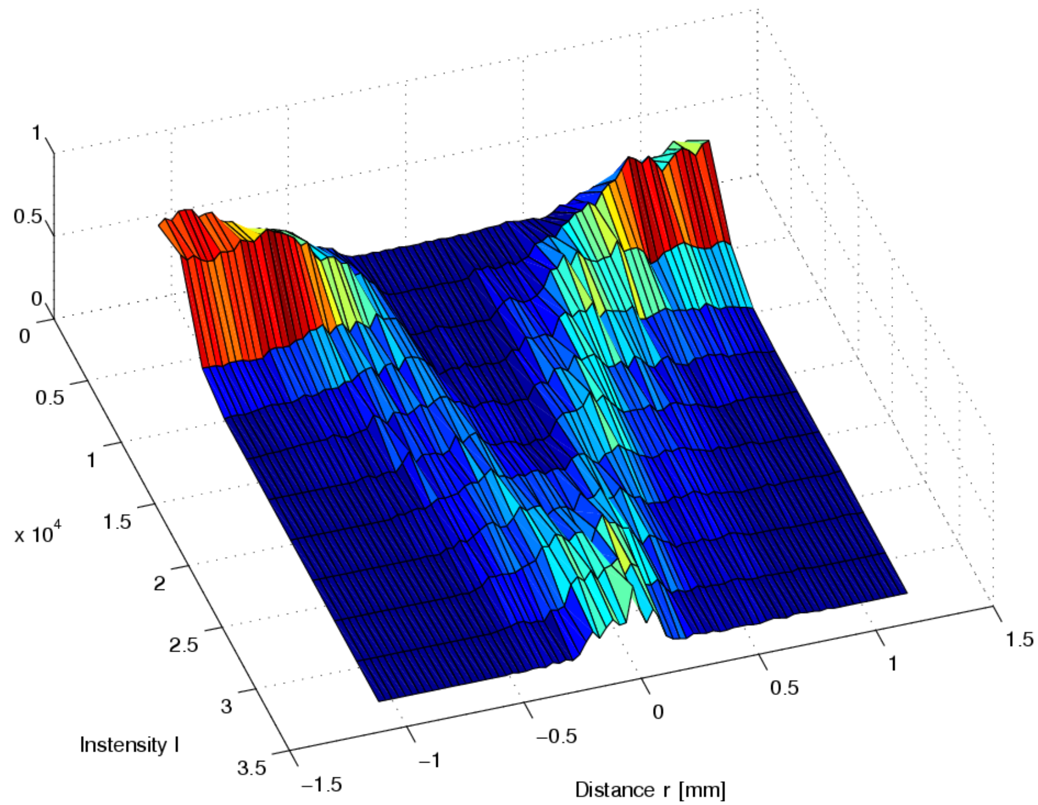

MODEL II – ESTIMATING MODEL PARAMETERS

- Parameter vector θ define polynomial approximating electrode axis $a(t;\theta)$,

$$\begin{aligned} x(t) &= a_0 + a_1 t + a_2 t^2 + a_3 t^3 \\ y(t) &= b_0 + b_1 t + b_2 t^2 + b_3 t^3 \\ z(t) &= c_0 + c_1 t + c_2 t^2 + c_3 t^3,\ t \in \mathbb{R}, \end{aligned}$$

- θ is estimated using RANSAC algorithm.
  - Four randomly selected points define an axis model $a(t;\theta)$.
    - Points are discarded if curvature is too big.
  - Model quality:

$$Q(\theta) = \sum_{\vec{x}_i \in A_e} \log P(I(\vec{x}_i) \,|\, d(\vec{x}_i, a(t;\theta))),$$

    where $d(\vec{x}_i, a(t;\hat{\theta}))$ is an approximation of point-to-curve distance.
  - Number of iterations set so that

$$P[\text{missing-better-than-so-far-best model}] \leq 0.05.$$

    If better model is found number of iterations is adjusted.

MODEL II – OPTIMIZATION OF AXIS POSITION

- RANSAC estimate θ of axis is taken as a starting point.
- Using Nelder-Mead simplex method, we optimize:

$$C(\theta) = -\sum_{\vec{x}_i \in A_e} \log P(I(\vec{x}_i) \,|\, d(\vec{x}_i, a(t; \hat{\theta}))),$$

- Decrease in $C(\theta)$ is used as stop criterion.
- Possibility to include into RANSACE $\Rightarrow$ Lo-RANSAC.

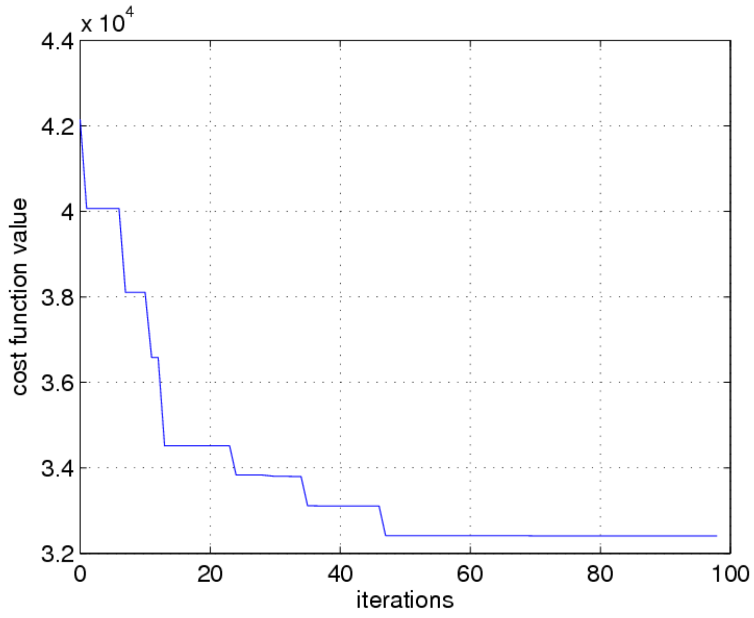

Electrode tip localization

TIP LOCALIZATION

- One tip needs to be localized.
- Voxel intensity is traced along estimated axis $a(t;\theta)$:

$$\gamma(t) = I(a(t;\theta)); \qquad \forall t \in \mathbb{R} : a(t;\theta) \in A.$$

- Tip is where $\gamma(t)$ falls under predefined threshold T.
- Estimated probabilities: $P(electrode \,|\, I)$, $P(background \,|\, I)$.
- Threshold T such that $P(electrode \,|\, T) = P(background \,|\, T)$.

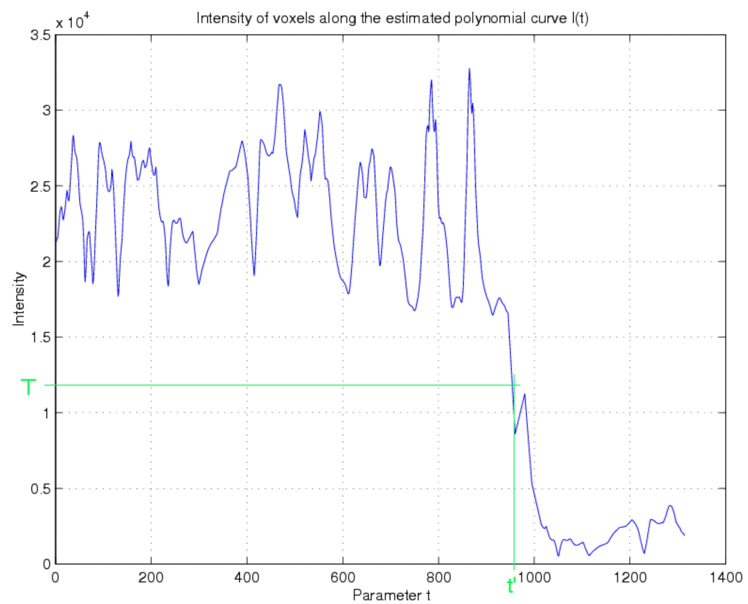

EXPERIMENTS – SIMULATED IMAGES

- Package FIELD II permits numerical simulation of RF signals.
- FIELD II parameters are set to imitate scanner Kretz Voluson 530D.
- 3D images were reconstructed from simulated RF signals.

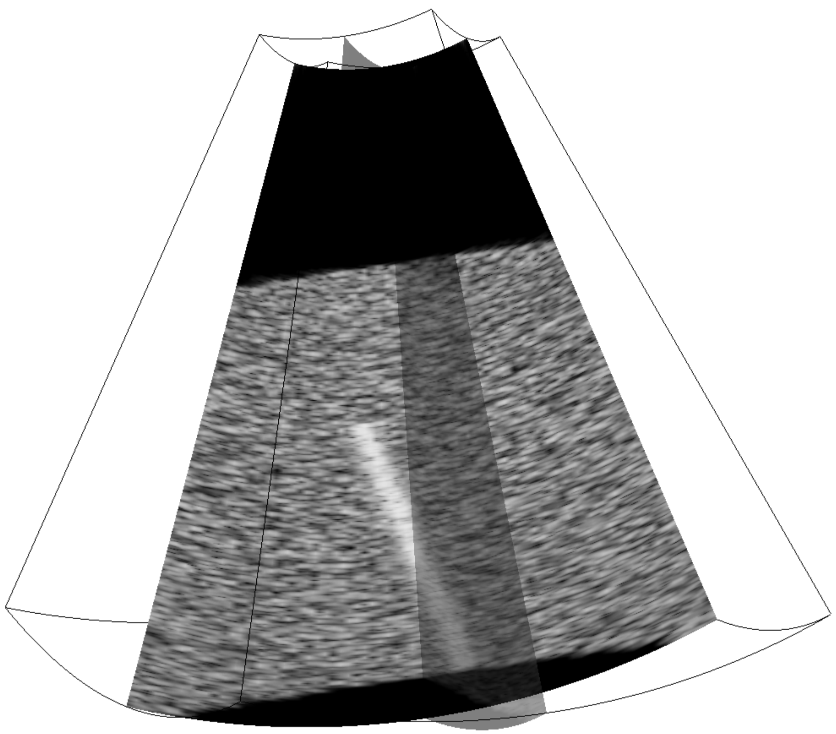

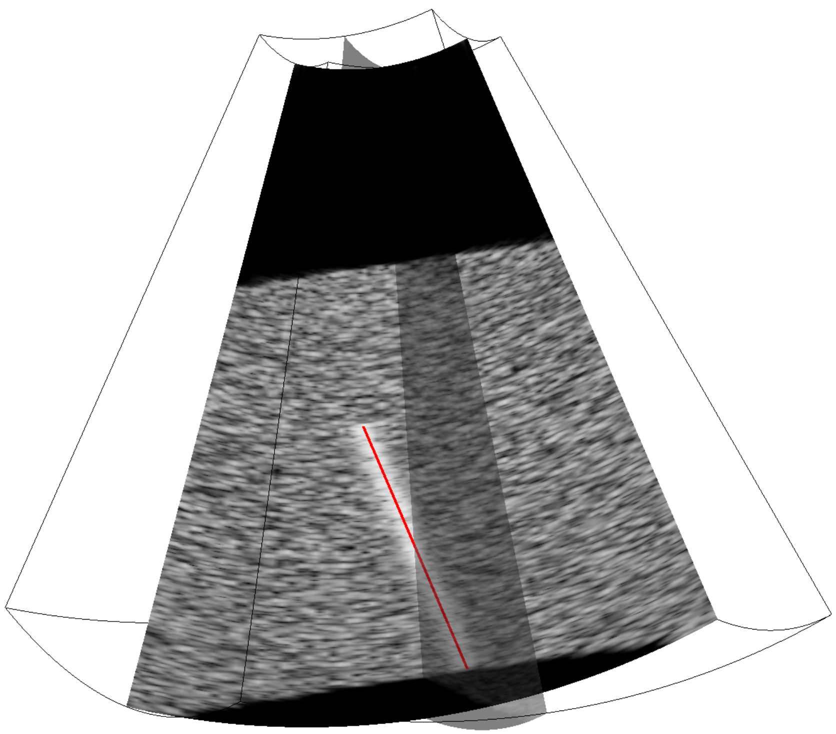

EXPERIMENTS – SIMULATED IMAGES

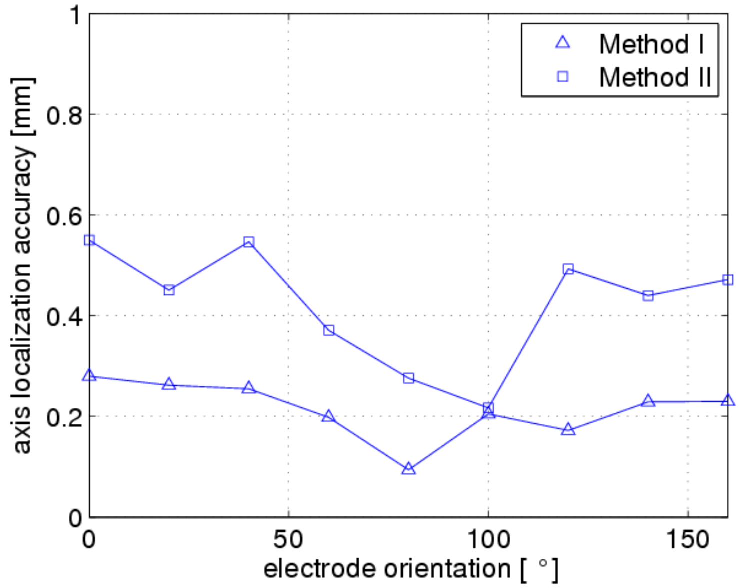

Axis accuracy – varying angle orientations.

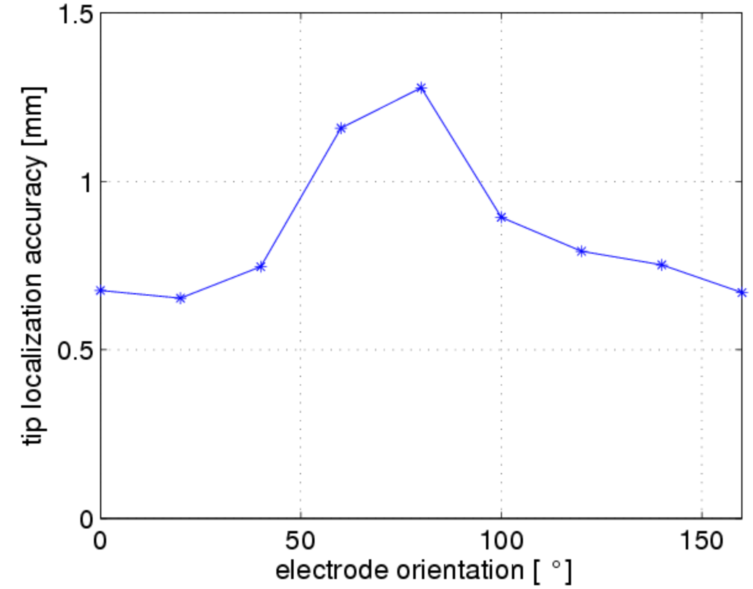

Tip accuracy – varying angle orientations.

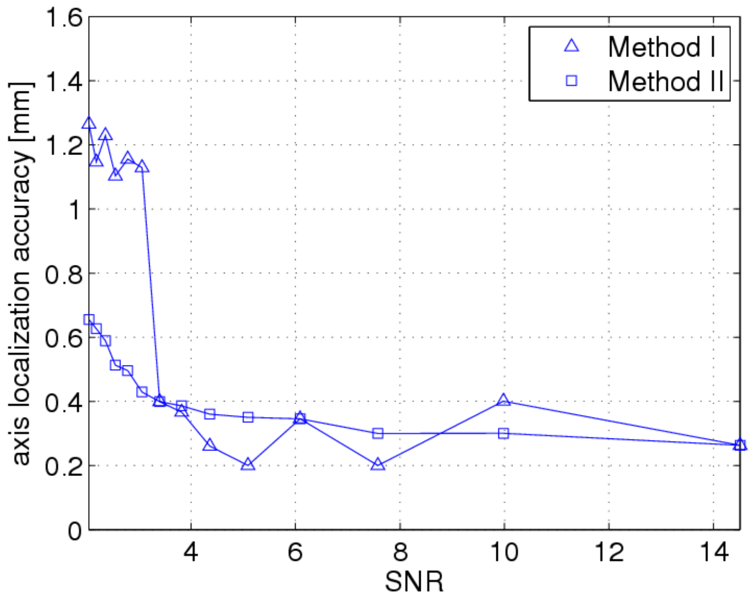

Axis accuracy – varying SNR.

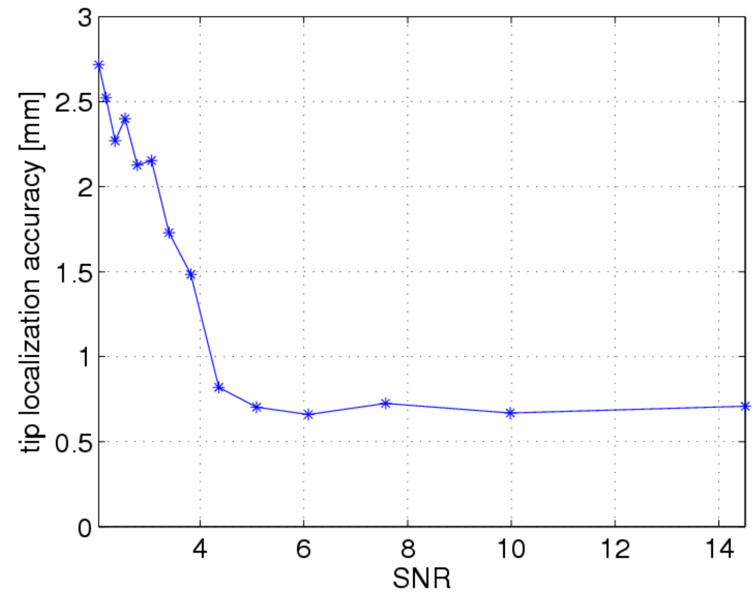

Tip accuracy – varying SNR.

EXPERIMENTS – REAL ULTRASOUND IMAGES

- Tungsten electrode (ϕ150 μm) inserted into polyvinyl cryogel alcohol (PVA) phantom.
- Phantom placed into water filled container.
- Scanner Kretz Voluson 530D equipped with RF output scanned the phantom.
- RF signals were stored to disk and 3D images were constructed offline.

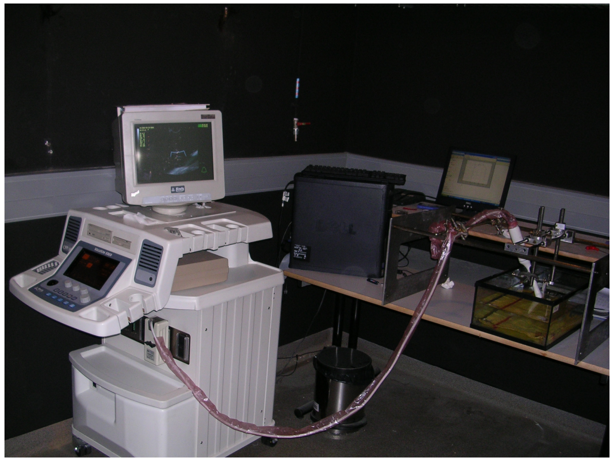

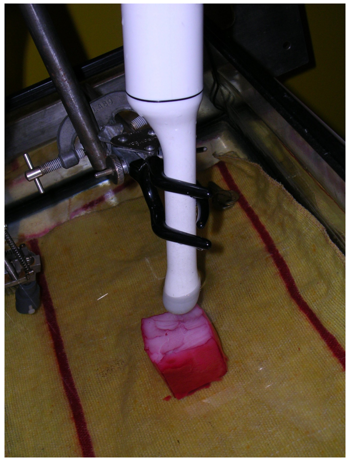

EXPERIMENTS – REAL ULTRASOUND IMAGES

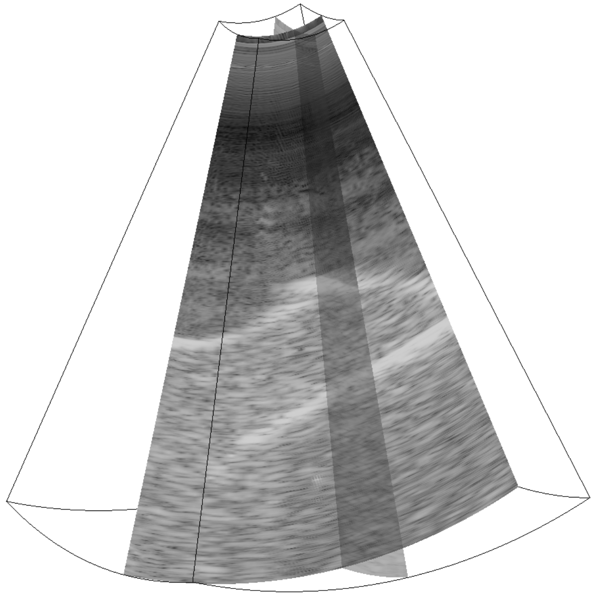

Real ultrasound image of PVA phantom.

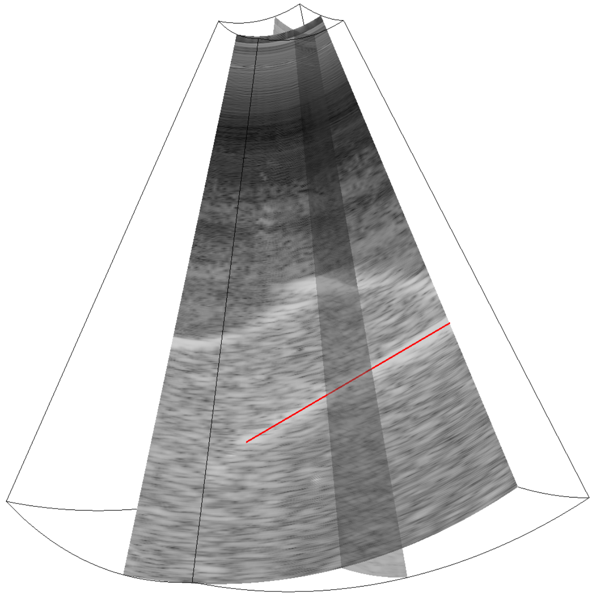

Localized electrode axis and tip.

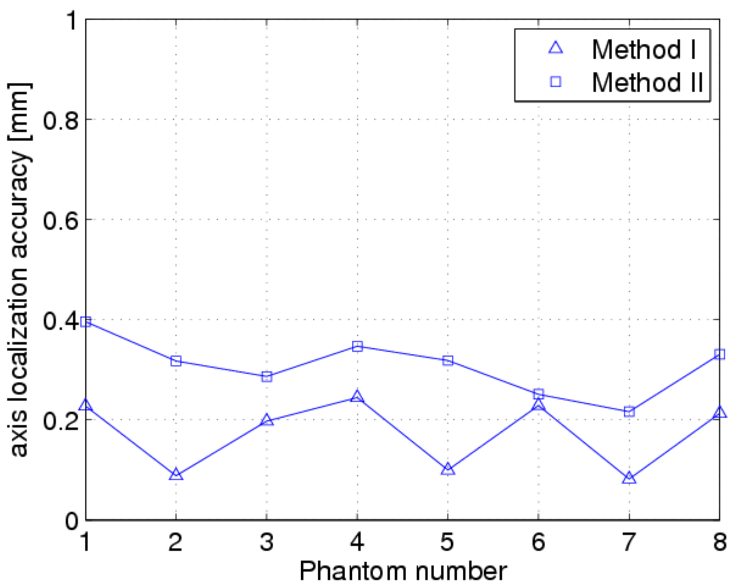

Axis accuracy.

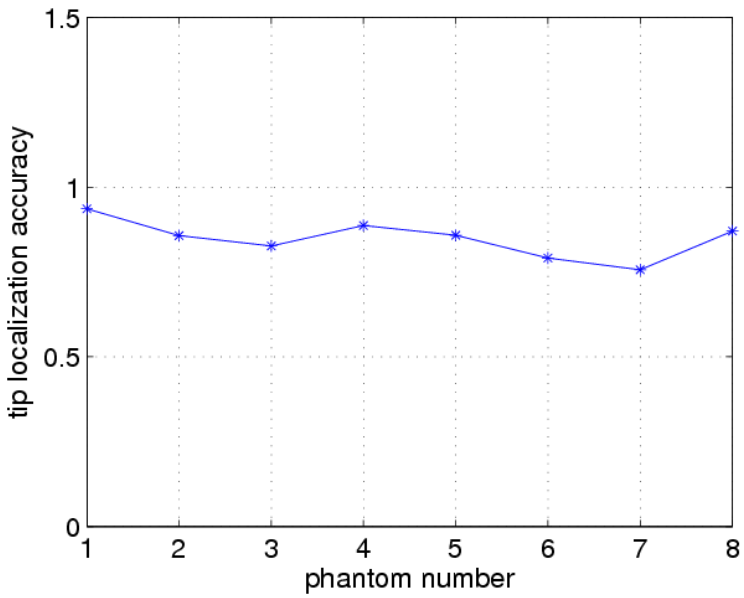

Tip accuracy.

CONCLUSIONS

- Novel methods for electrode localization in 3D ultrasound images:
  - Method I – Parallel Integral Projection
    - + Robust to noise.
    - + Can handle discontinuous axis.
    - + Few a priori assumptions about electrode.
    - - Problem with curvilinear axis.
    - - Computational in tens of minutes.
  - Method II – RANSAC-based model fitting
    - + Robust to noise.
    - + Can handle discontinuous axis.
    - + Estimation of electrode with curvilinear axis is possible.
    - + Fast processing permits near real time localization.
    - - Need for training data to deduce statistical models.
  - Tip localization
    - + Optimized using intensity priors.
    - - Sensitivity to electrode disruptions.
- Tested on simulated and real ultrasound data.
- Accuracy on order of hundreds μm.

Thank you for your attention and ...

PUBLICATIONS

- Martin Barva, Jean-Martial Mari, Jan Kybic, and Christian Cachard. Radial Radon transform for electrode localization in biological tissue. In Jiří Jan, Jiří Kozumplík, and Ivo Provazník, editors, BIOSIGNAL : Analysis of Biomedical Signals and Images, pages 299-301, Brno, Czech Republic, June 2004.
- Martin Barva, Jan Kybic, Jean-Martial Mari, and Christian Cachard. Radial Radon transform dedicated to micro-object localization from radio frequency ultrasound signal. In Marjorie Passini Yuhas, editor, IEEE UFFC : Proceedings of the IEEE International Frequency Control Symposium and Exposition, pages 1836-1839, Montreal, Canada, August 2004.
- Martin Barva. Automatic object localization from 3D ultrasound data (Ph.D. thesis proposal). Research Report CTU-CMP-2005-04, Center for Machine Perception, K13133 FEE Czech Technical University, Prague, Czech Republic, February 2005.
- Martin Barva, Jan Kybic, Jean-Martial Mari, Christian Cachard, and Václav Hlaváč. Automatic localization of curvilinear object in 3D ultrasound images. SPIE International Symposium on Medical Imaging, San Diego, California, February 2005.
- Martin Barva, Jan Kybic, Jean-Martial Mari, Christian Cachard, and Václac Hlaváč. Localizing metal electrode from 3D ultrasound data using RANSAC and intensity priors. IFMBE Proceedings EMBEC05, 3rd European Medical and Biological Engineering Conference, November, Prague, Czech Republic, 2005.
- Martin Barva and Jan Kybic and Hervé Liebgott and Christian Cachard and Václav Hlaváč, Comparison of methods for tool localization in biological tissue from 3D ultrasound data. IEEE UFFC : Proceedings of IEEE International Ultrasonics Symposium, Vancouver, Canada, August 2006. (in print)
- Martin Barva, Jan Kybic, Jean-Martial Mari, Jean-René Duhamel, Christian Cachard, Václav Hlaváč. Parallel Integral Projection Transform for medical tool localization in 3D ultrasound images, Journal of Ultrasonic Imaging. (preparing)

m p

Creatis

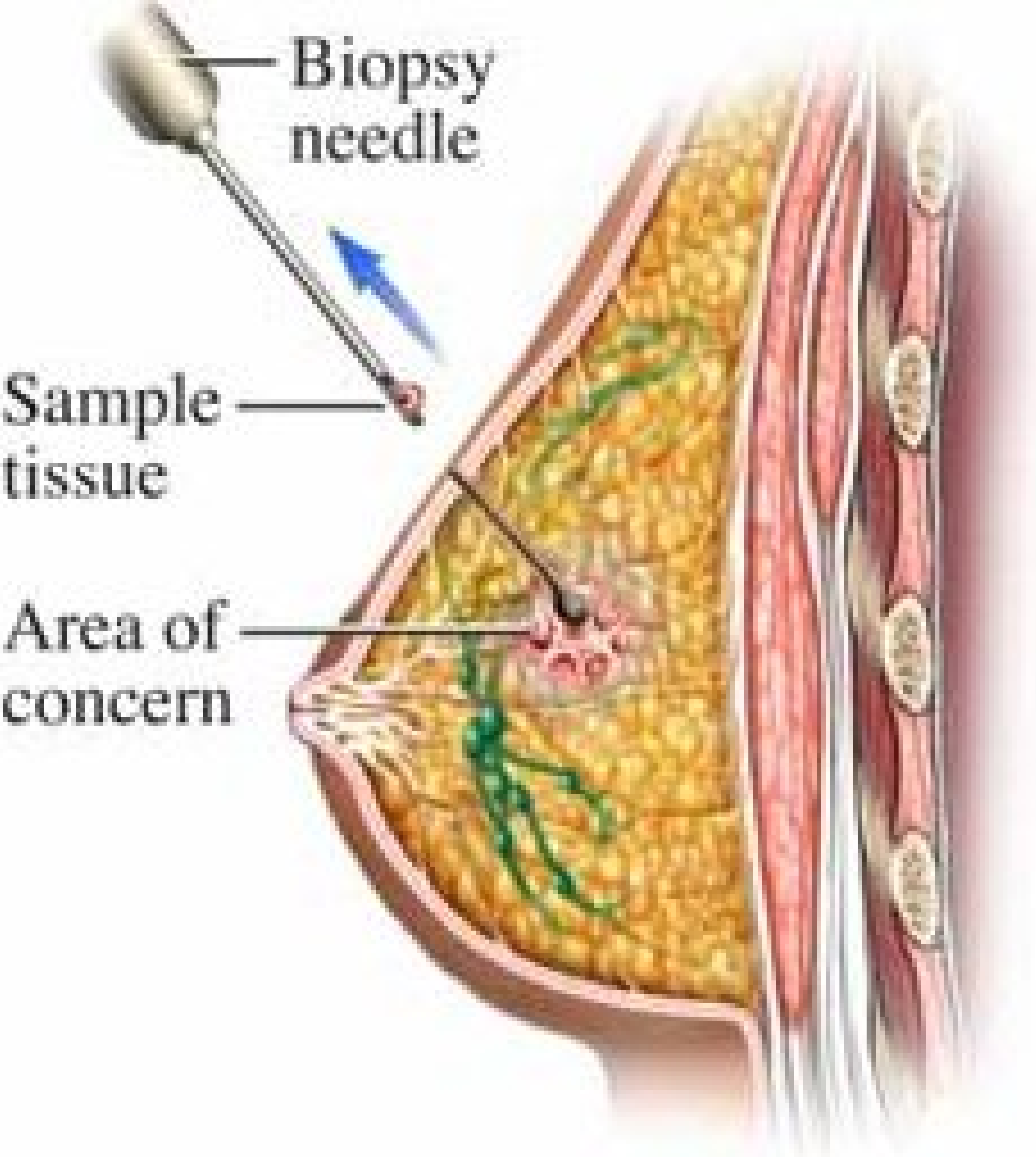
Biopsy needle
Sample tissue
Area of concern

Laparoscopy

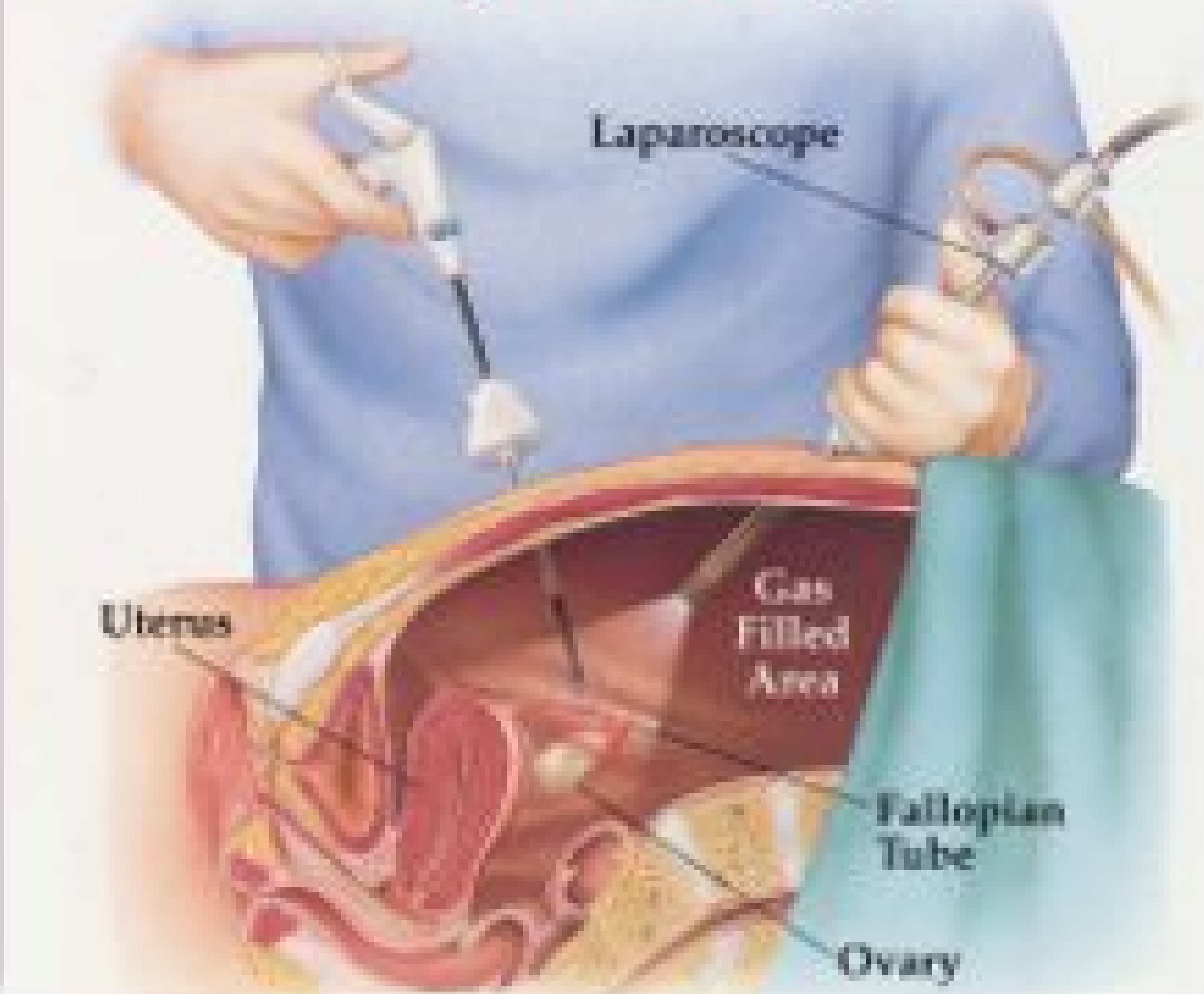

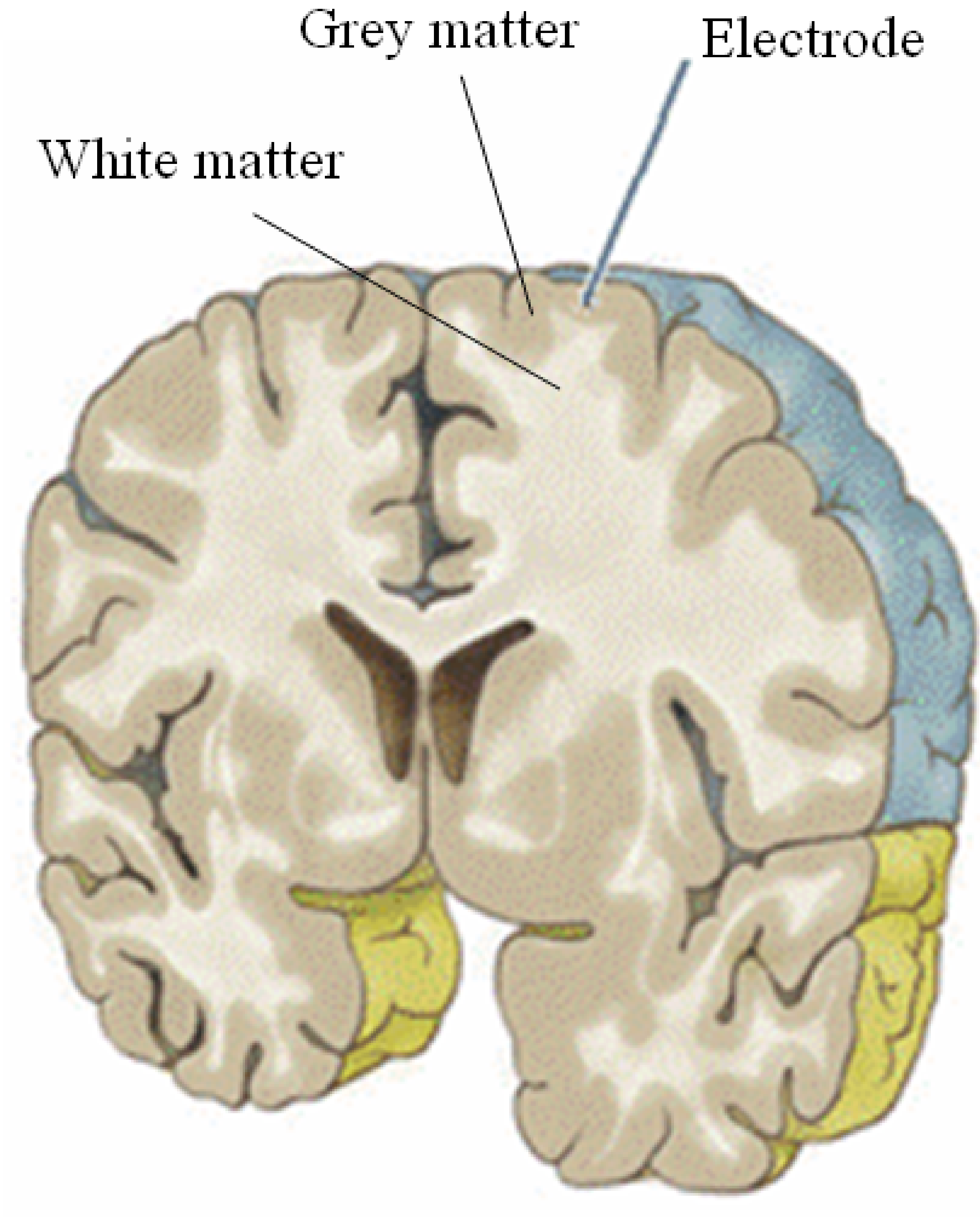

Sectional cortex area

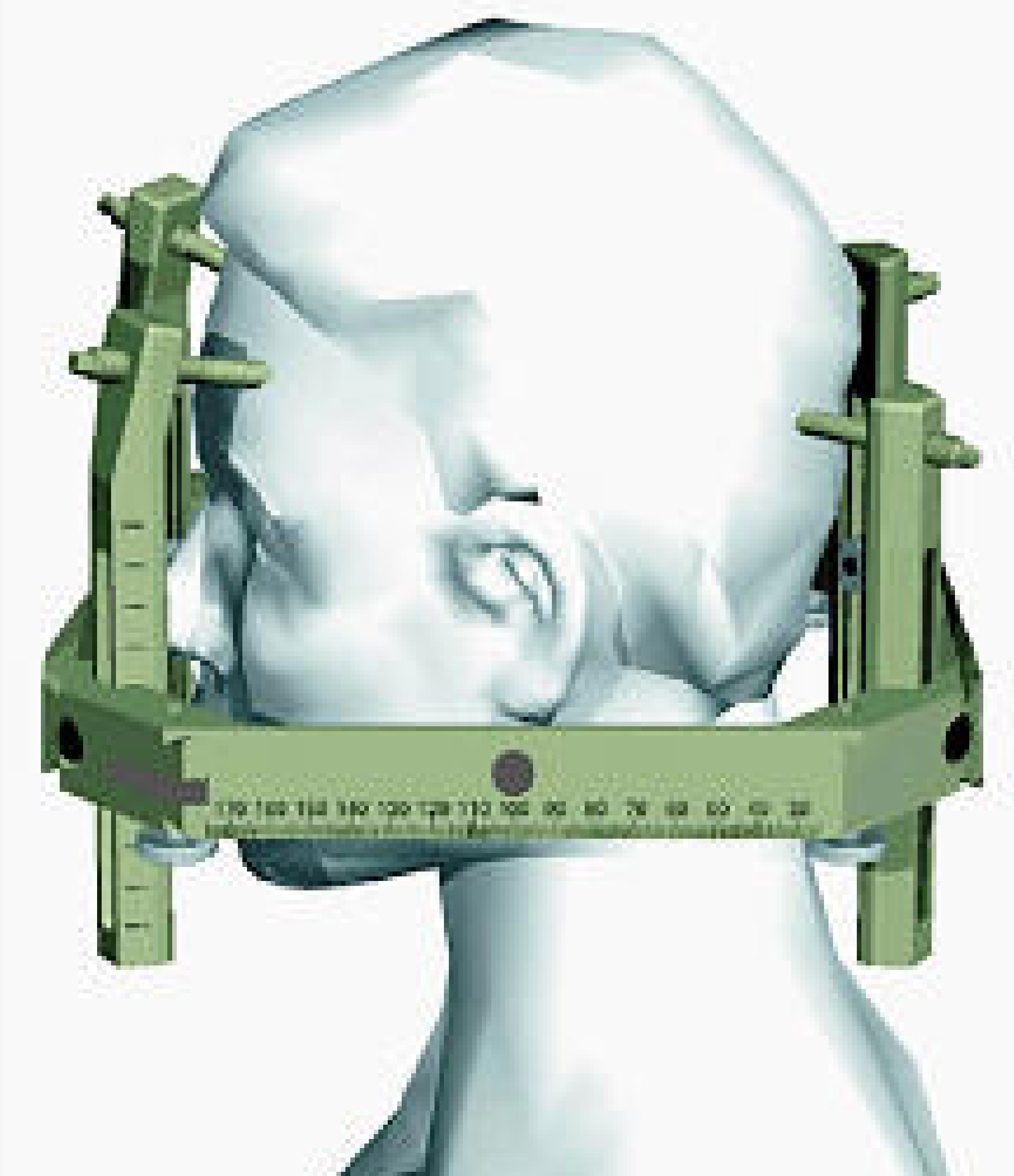

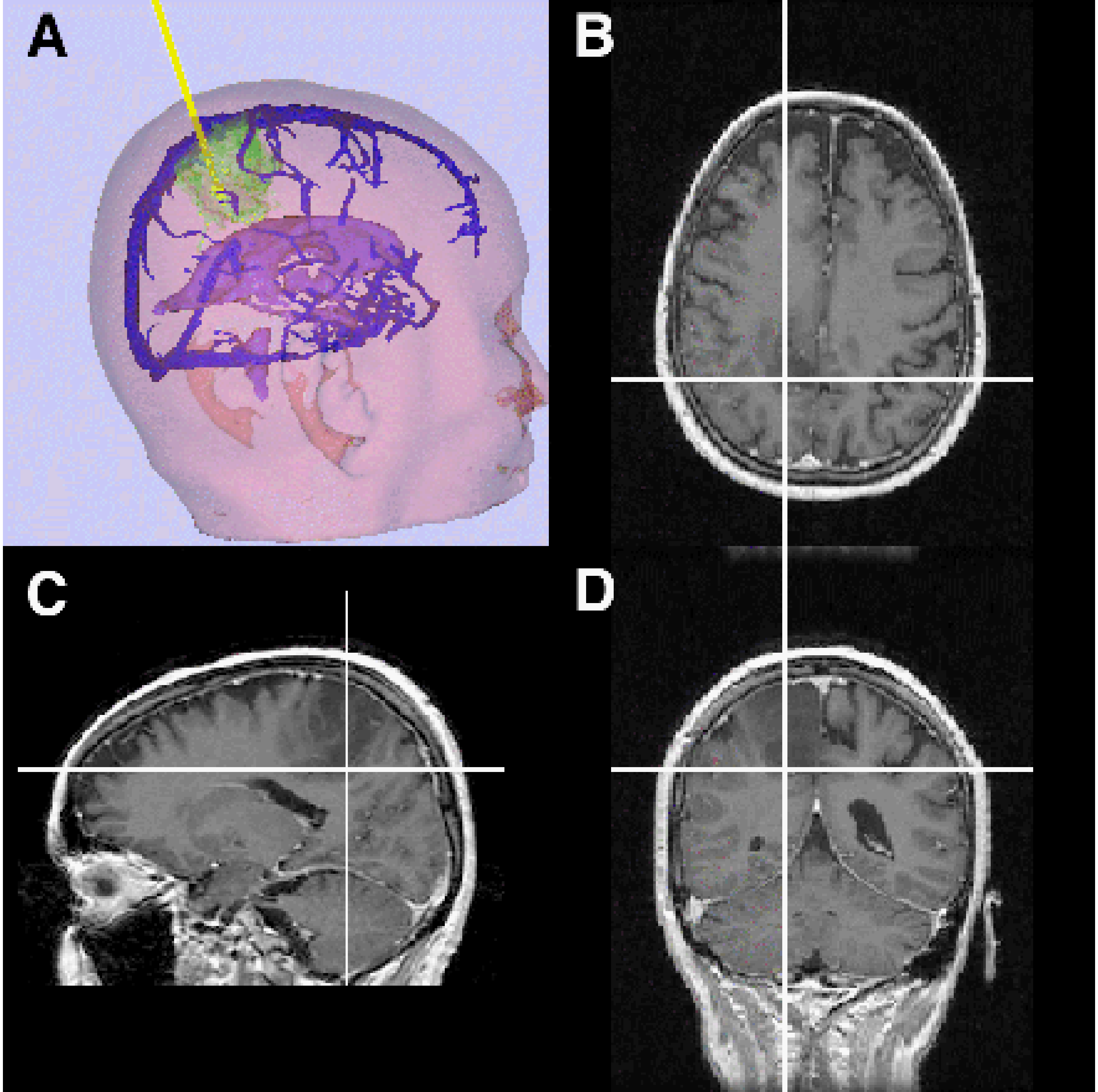
A
B
C
D

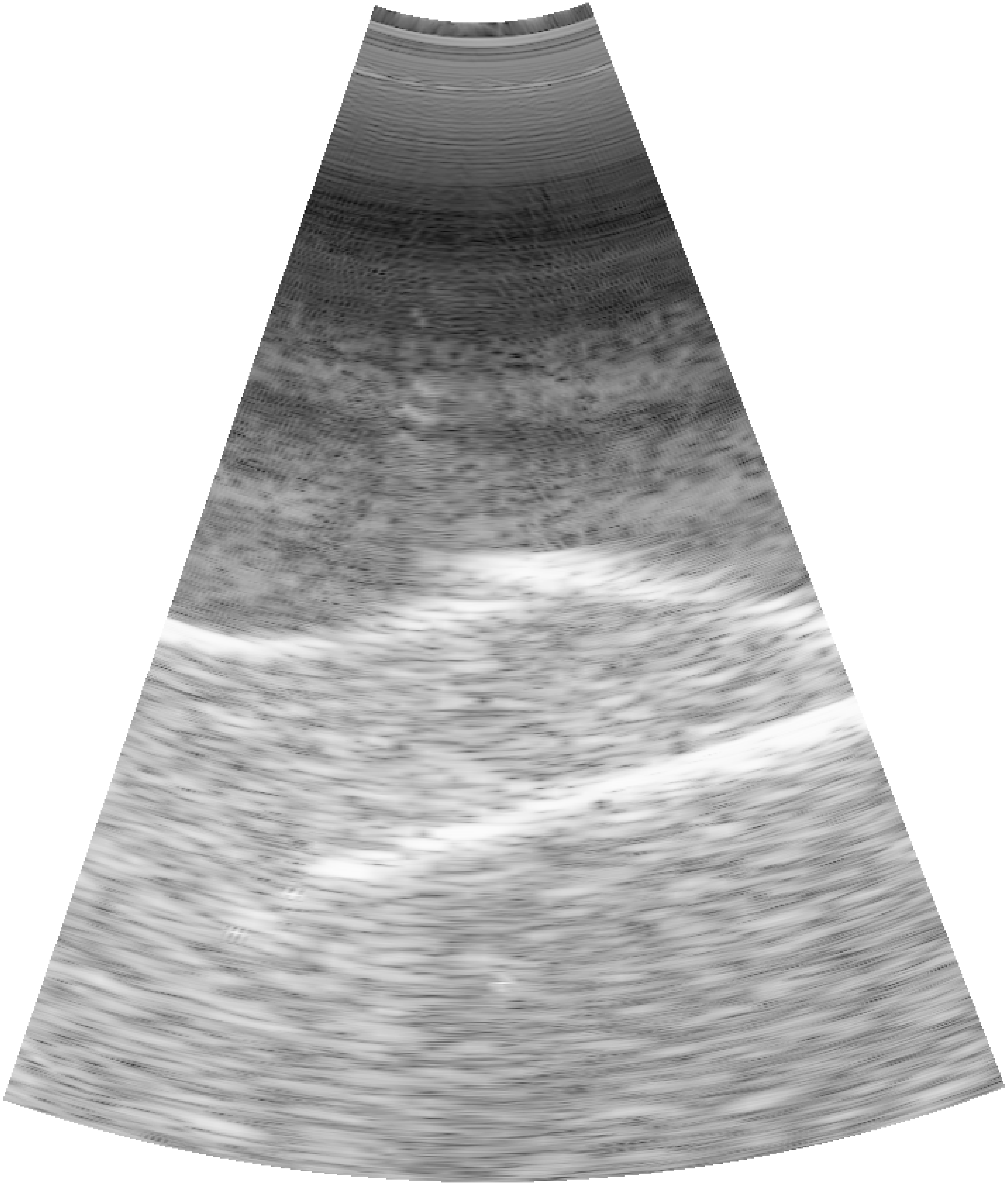

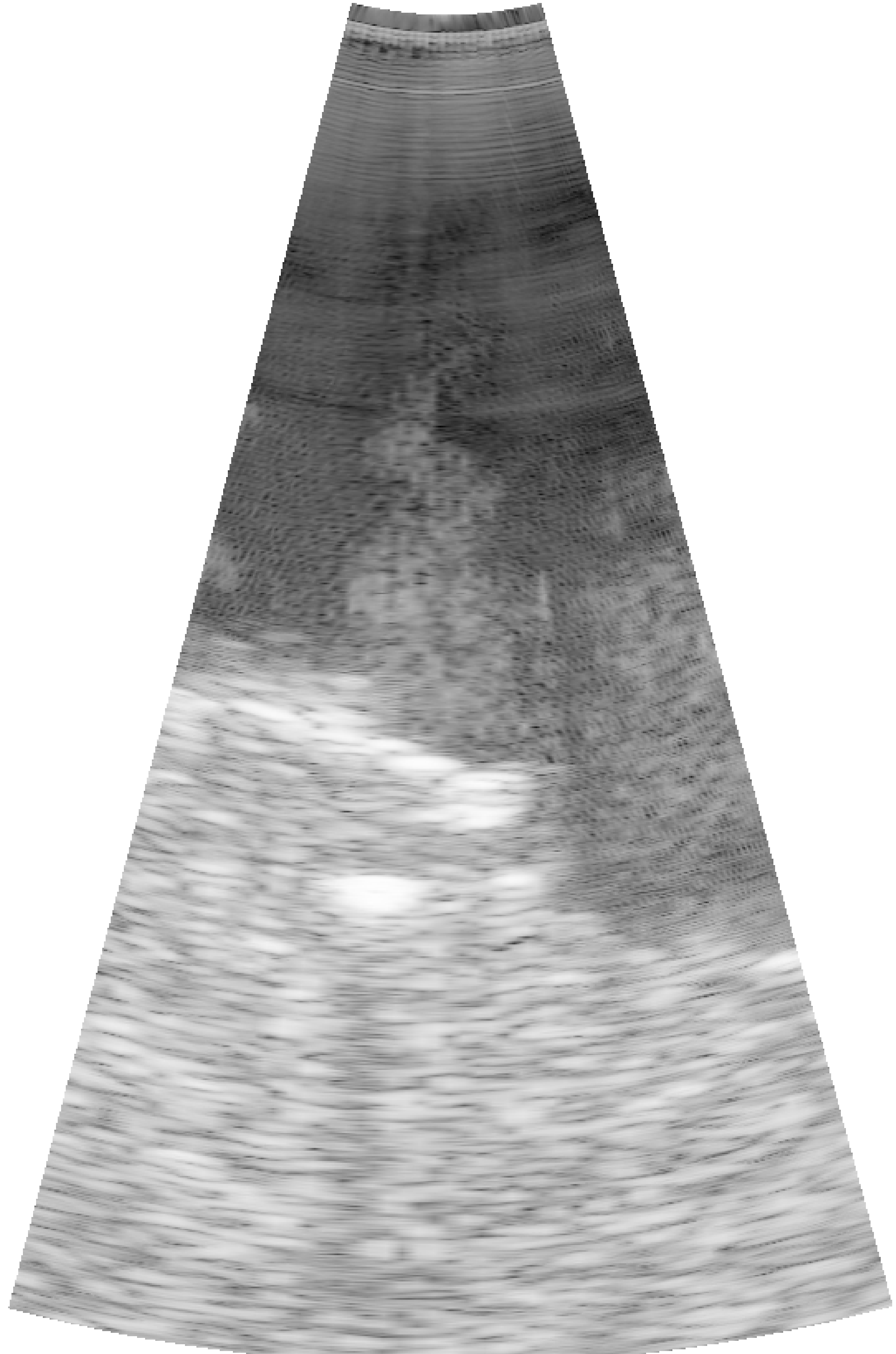

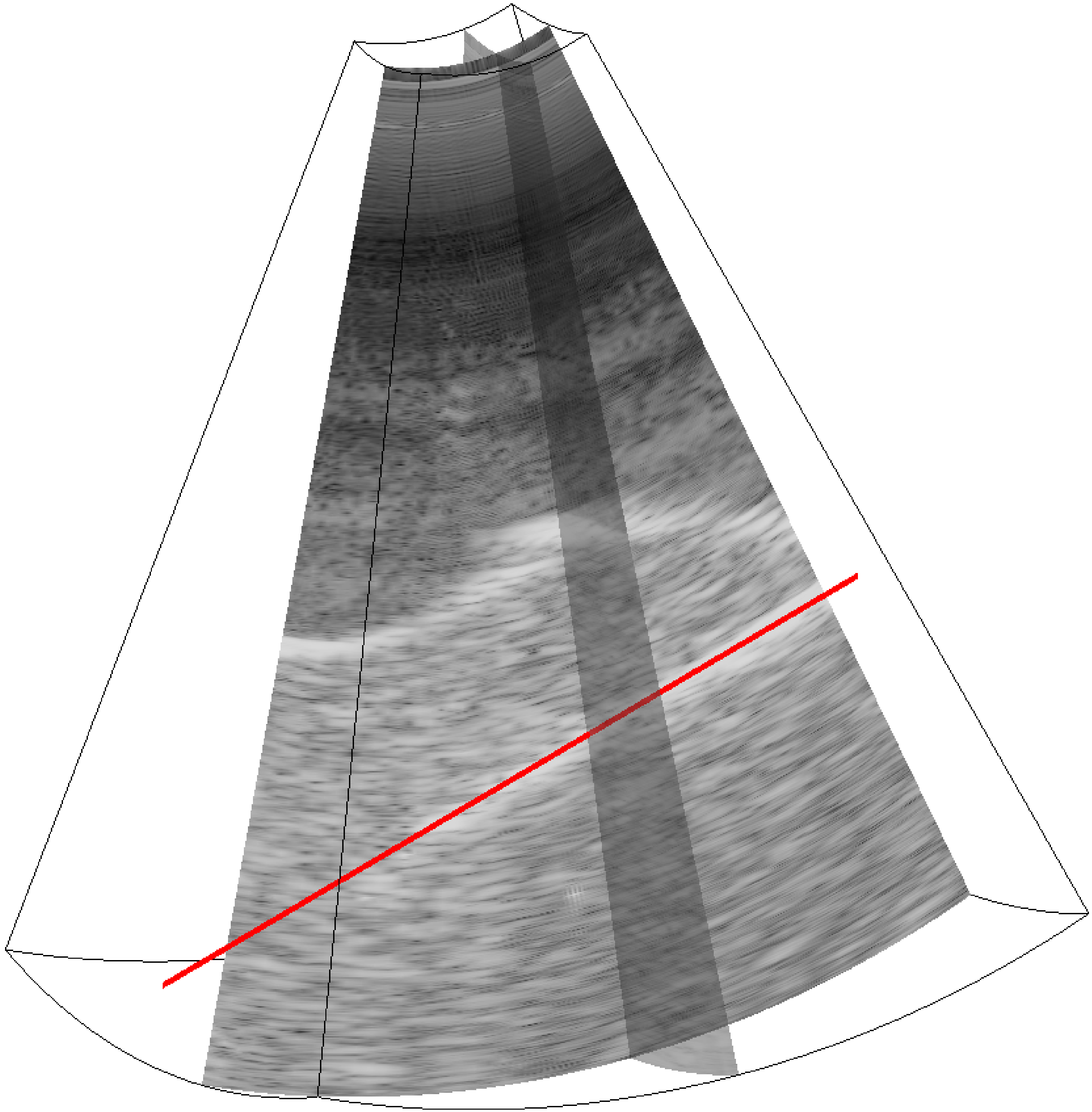

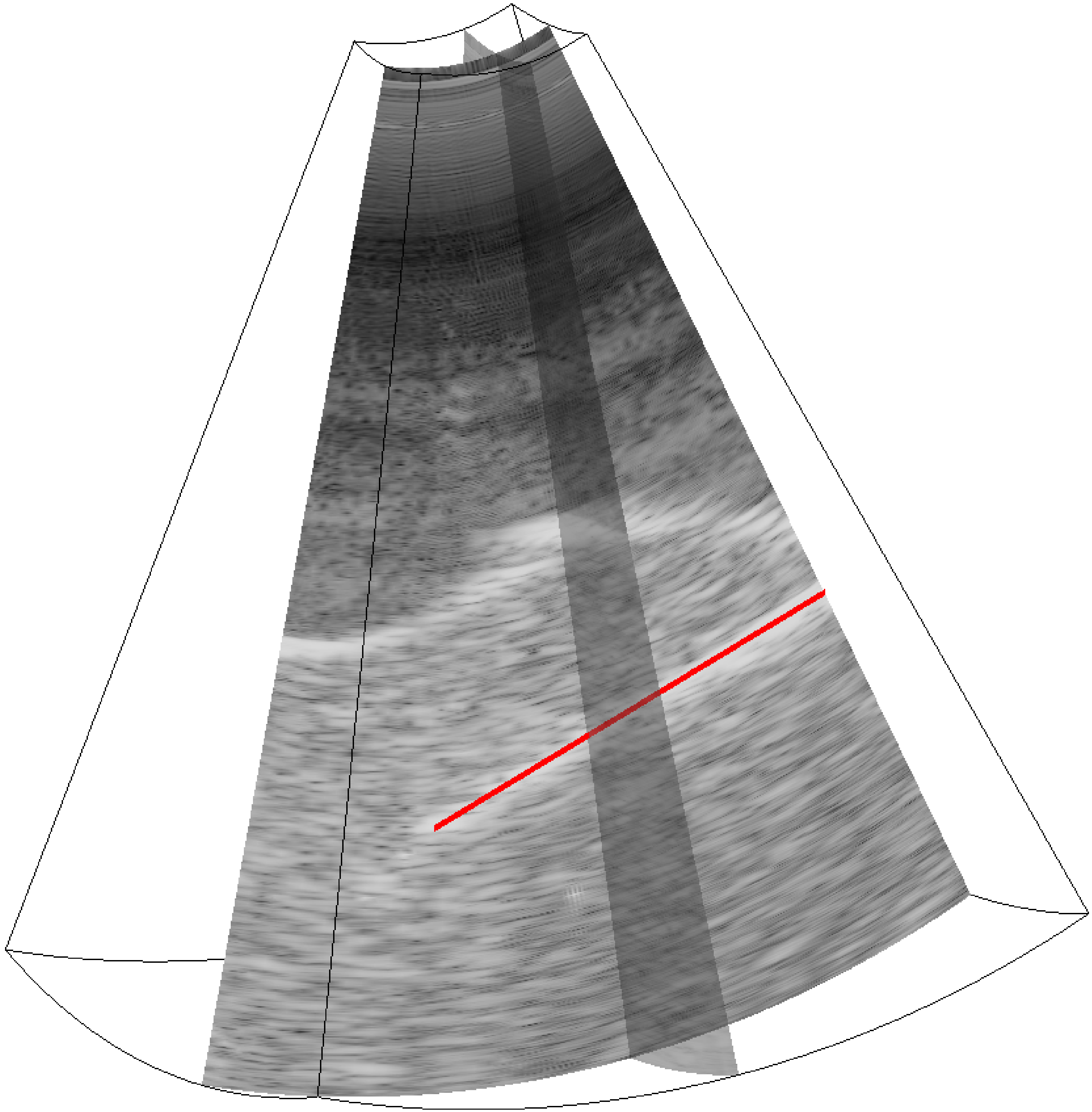

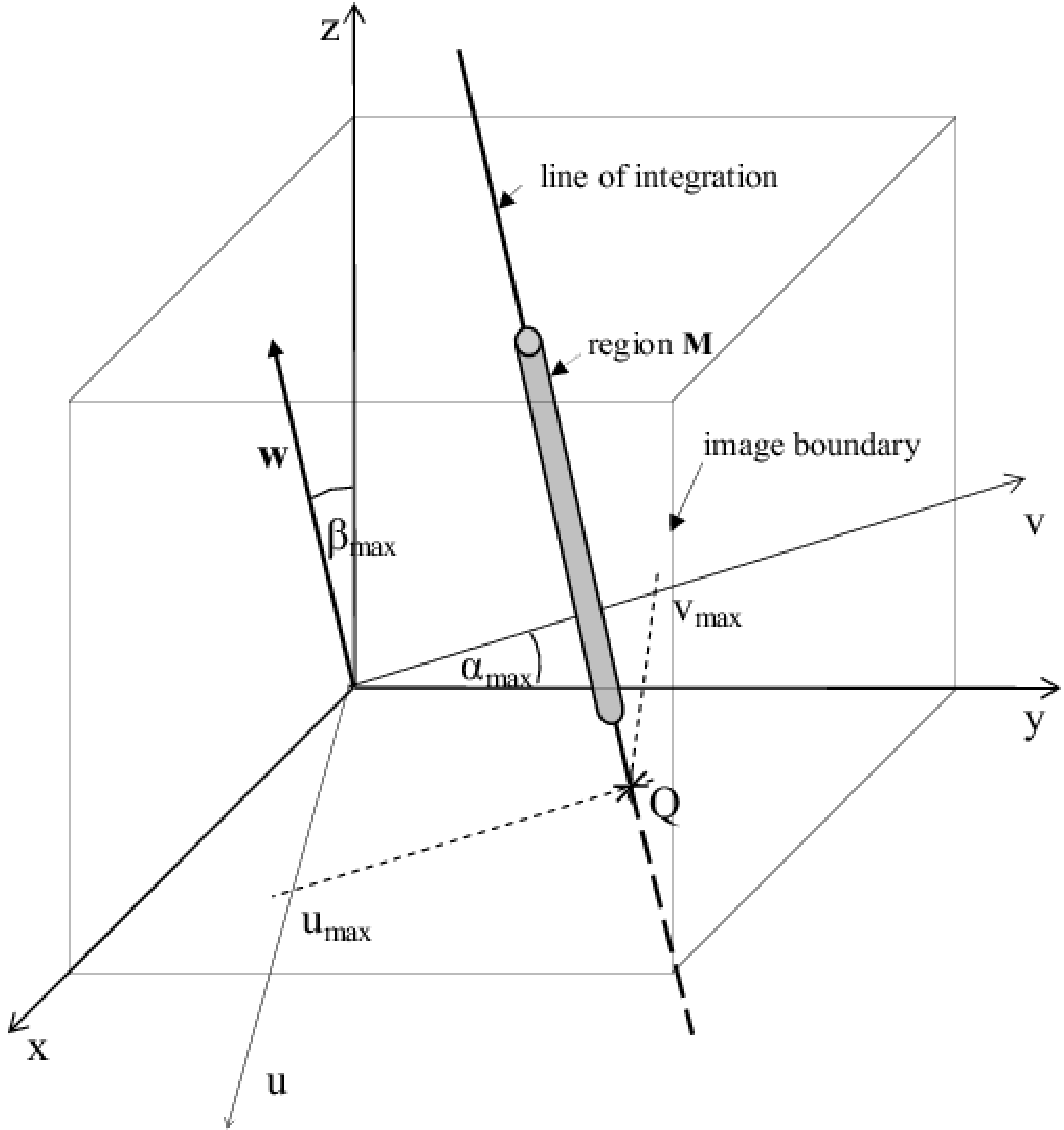

z
line of integration
region M
w
image boundary
v
βmax
vmax
αmax
y
Q
umax
x
u

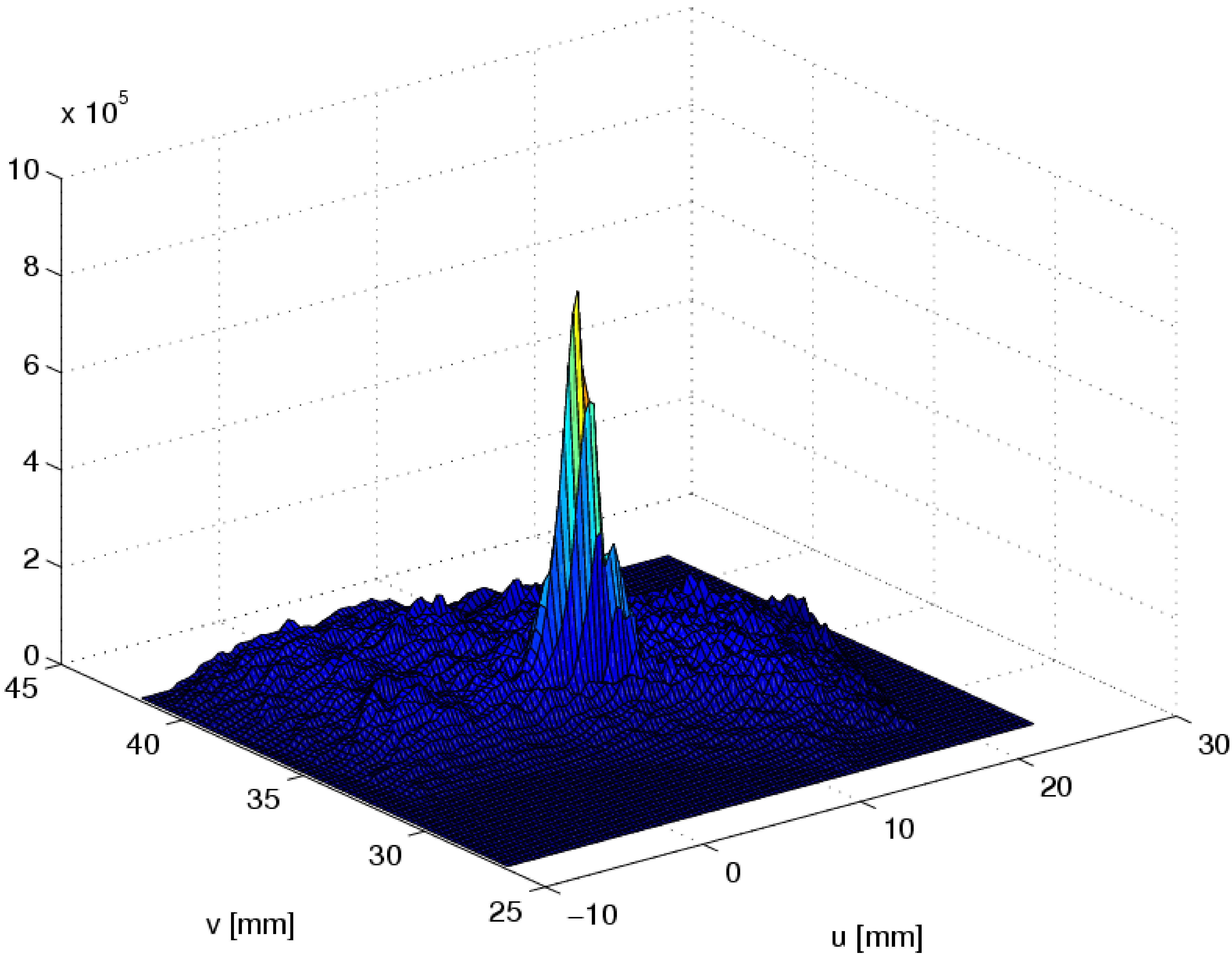
x 10^5
10
8
6
4
2
0
45
40
35
30
25
v [mm]
−10
0
10
20
30
u [mm]

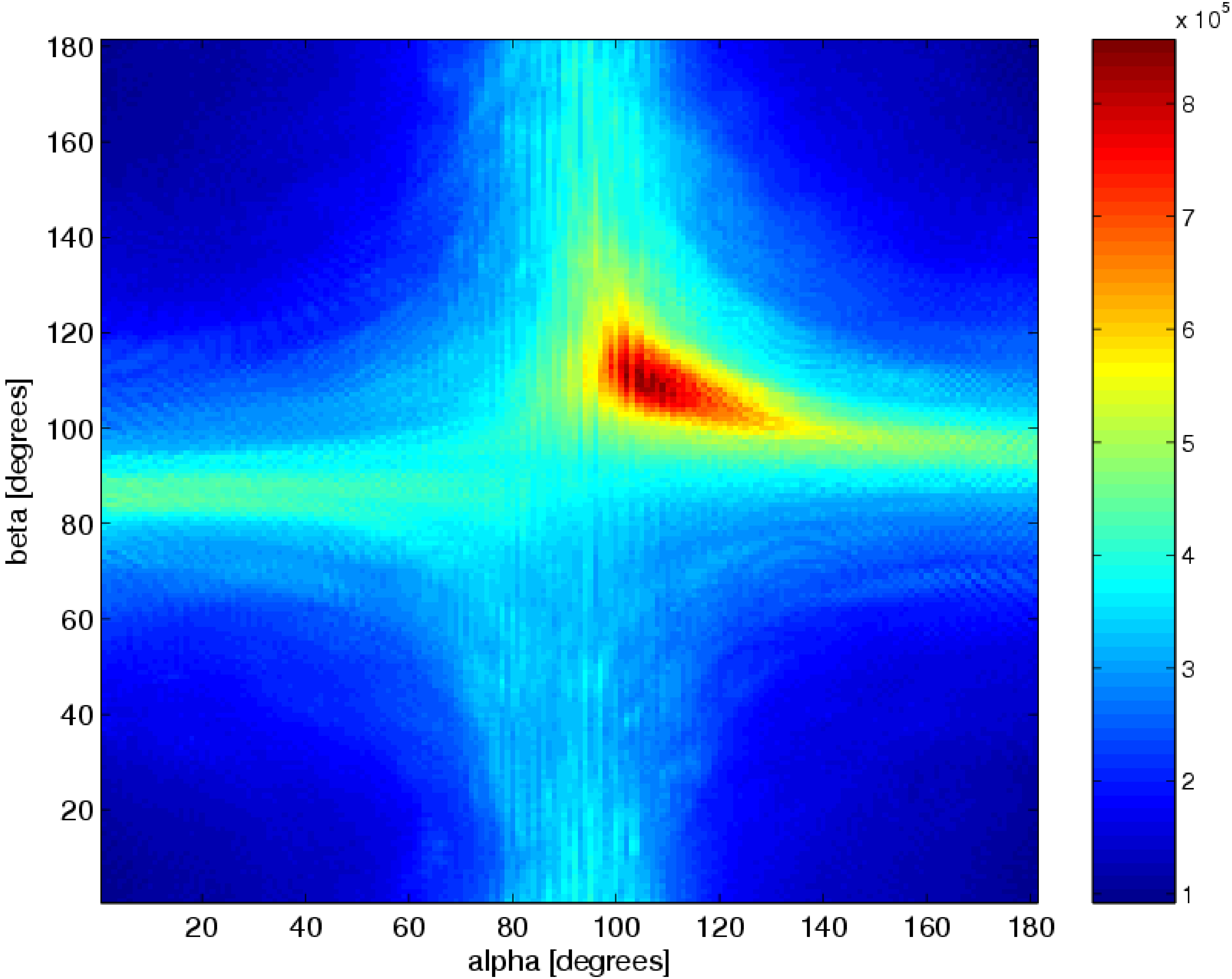
x 10^5
180
160
140
120
100
80
60
40
20
beta [degrees]
20
40
60
80
100
120
140
160
180
alpha [degrees]
8
7
6
5
4
3
2
1

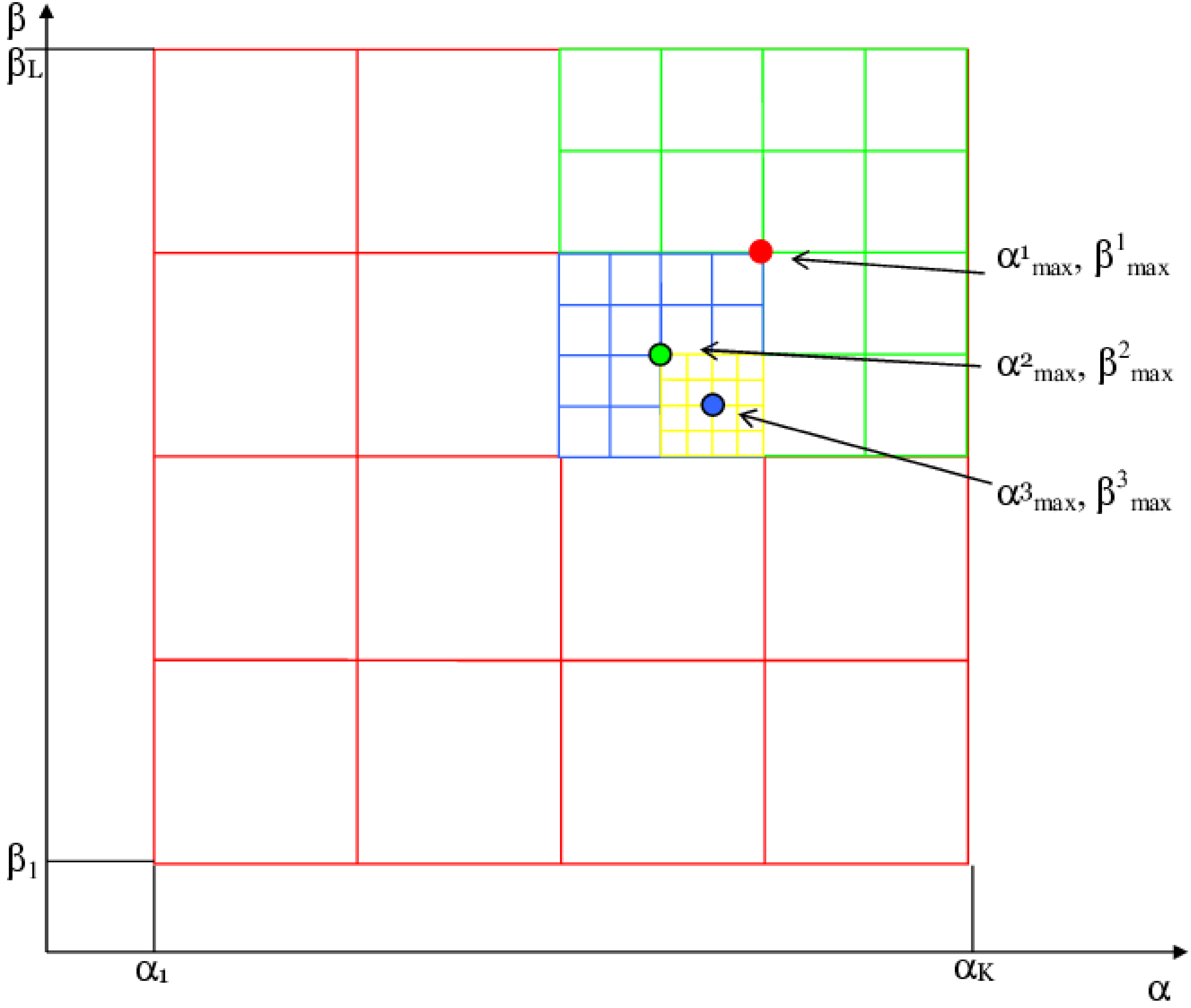
β
β_L
β_1
α_1
α_K
α
α¹max, β¹max
α²max, β²max
α³max, β³max

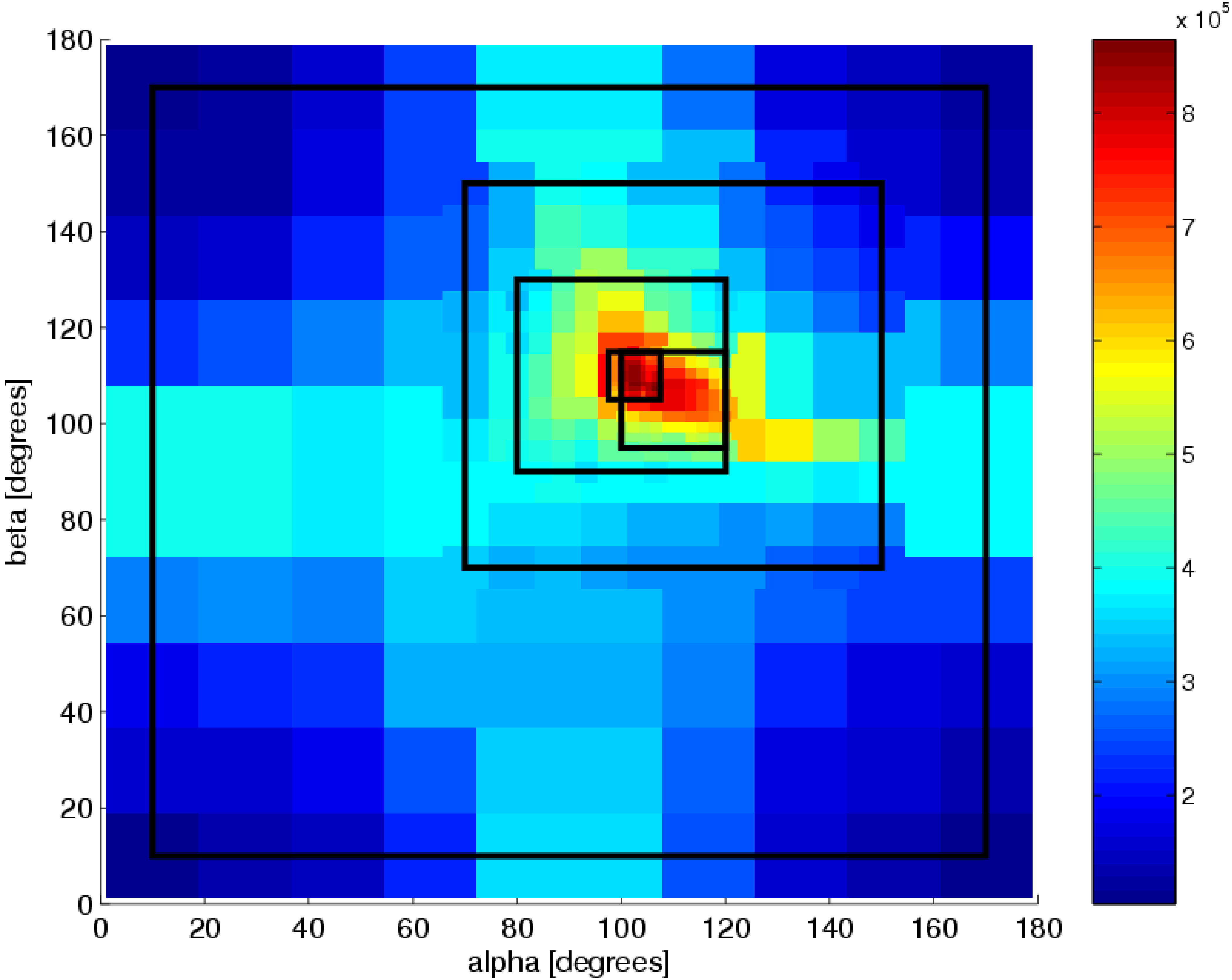

x 10^5
8
7
6
5
4
3
2
beta [degrees]
180
160
140
120
100
80
60
40
20
0
0
20
40
60
80
100
120
140
160
180
alpha [degrees]

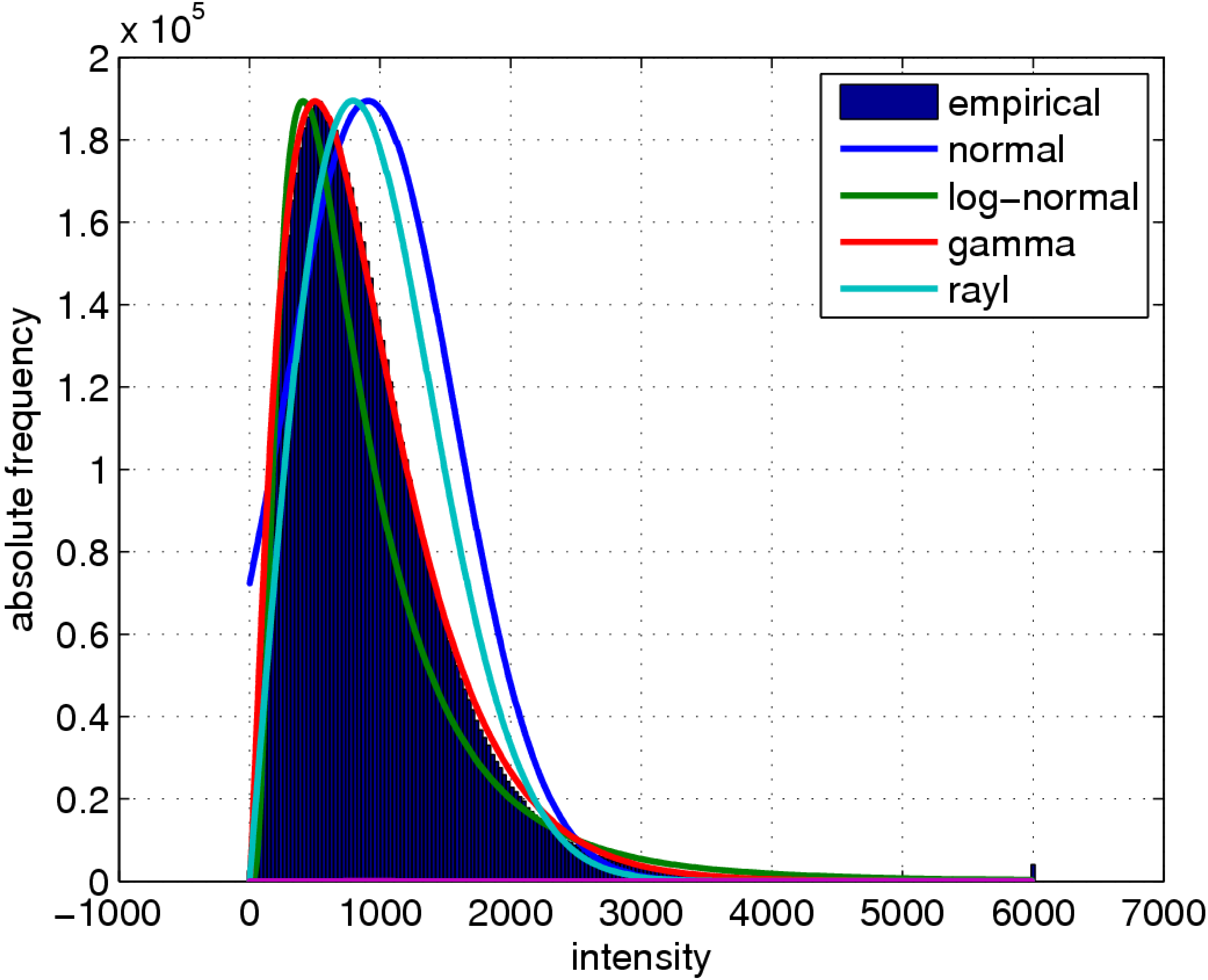
x 10^5
2
1.8
1.6
1.4
1.2
1
0.8
0.6
0.4
0.2
0
−1000
0
1000
2000
3000
4000
5000
6000
7000
intensity
absolute frequency
empirical
normal
log−normal
gamma
rayl

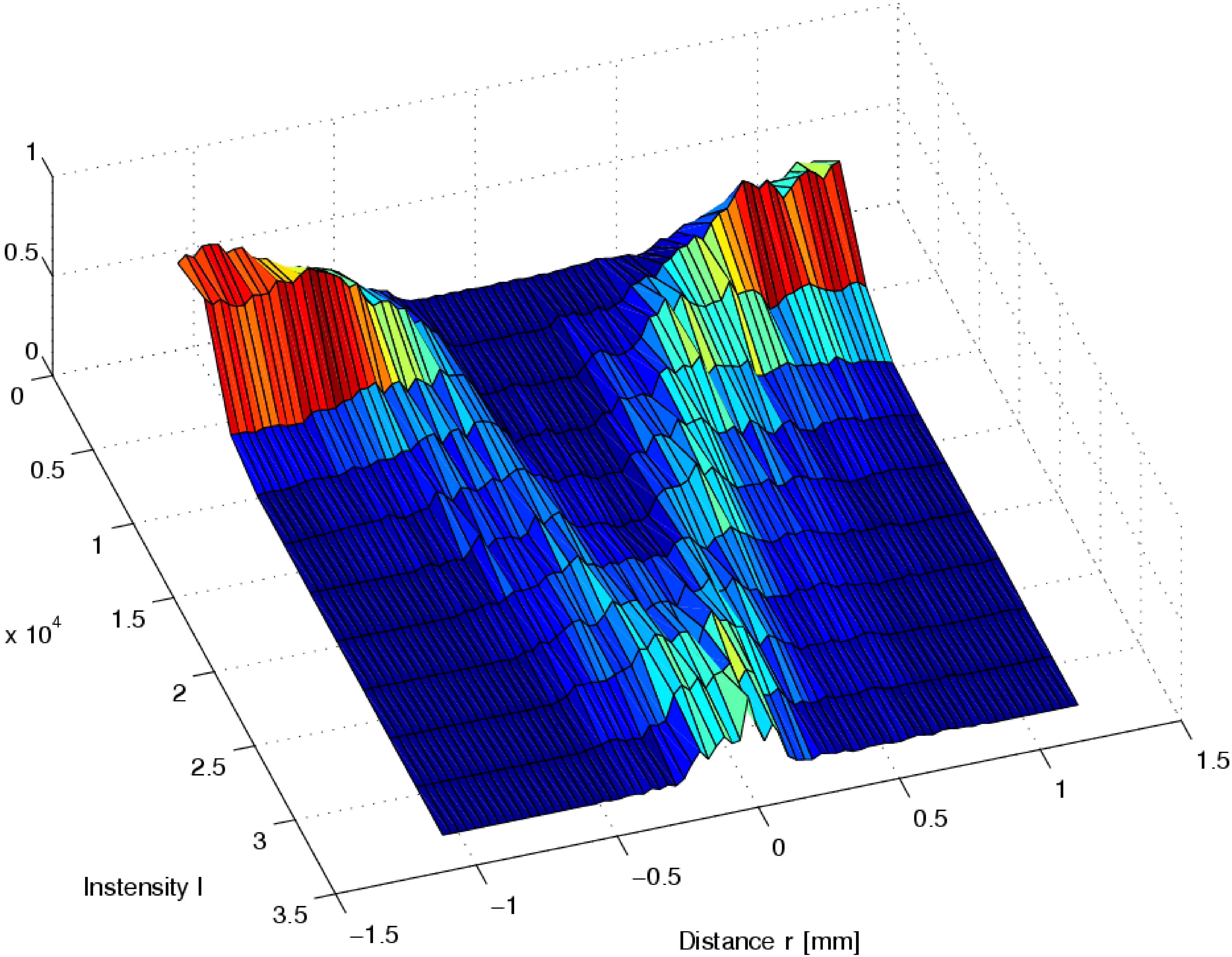

1
0.5
0
0
0.5
1
1.5
x 10^4
2
2.5
3
Instensity I
3.5
−1.5
−1
−0.5
0
0.5
1
1.5
Distance r [mm]

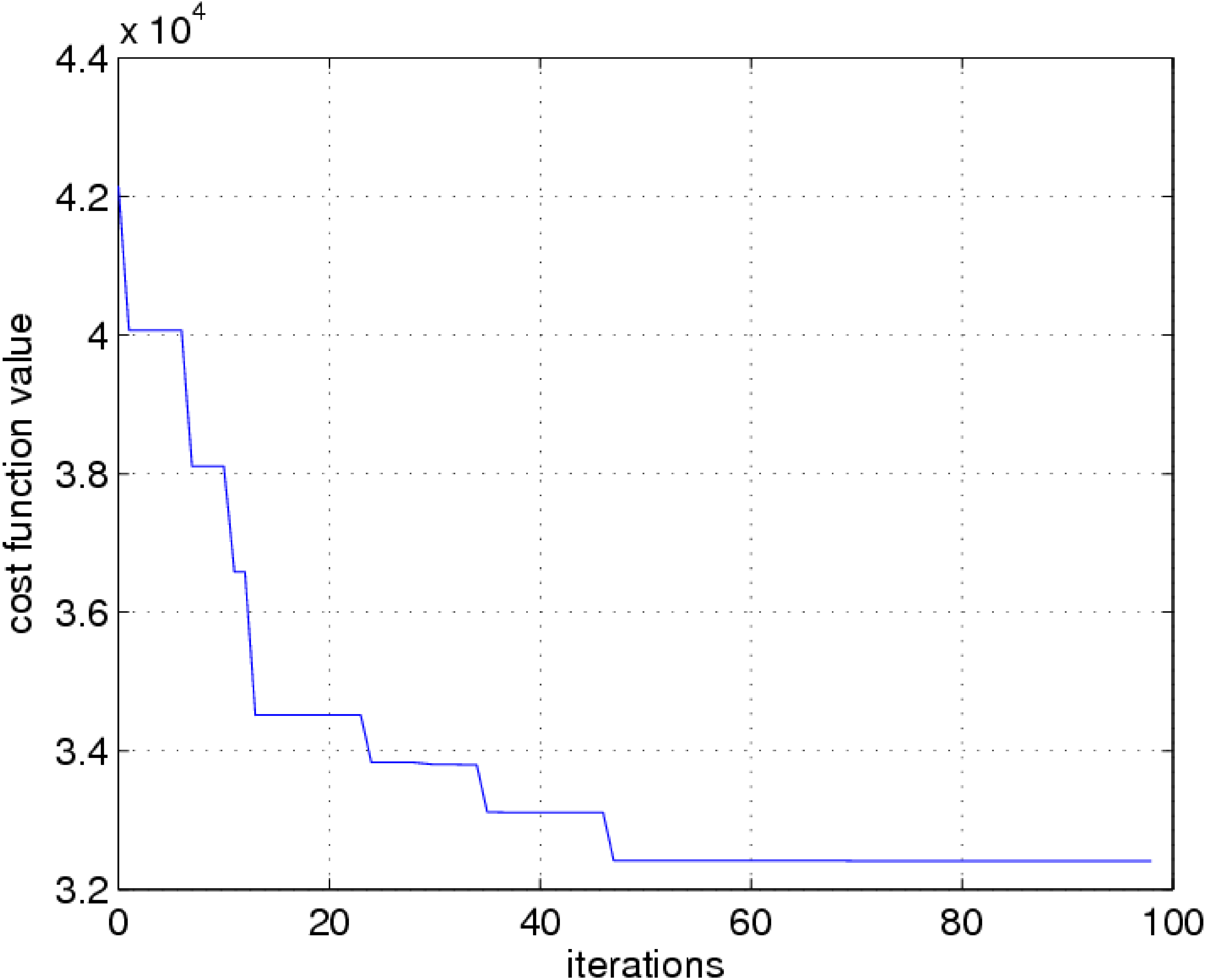
x 10^4
4.4
4.2
4
3.8
3.6
3.4
3.2
cost function value
0
20
40
60
80
100
iterations

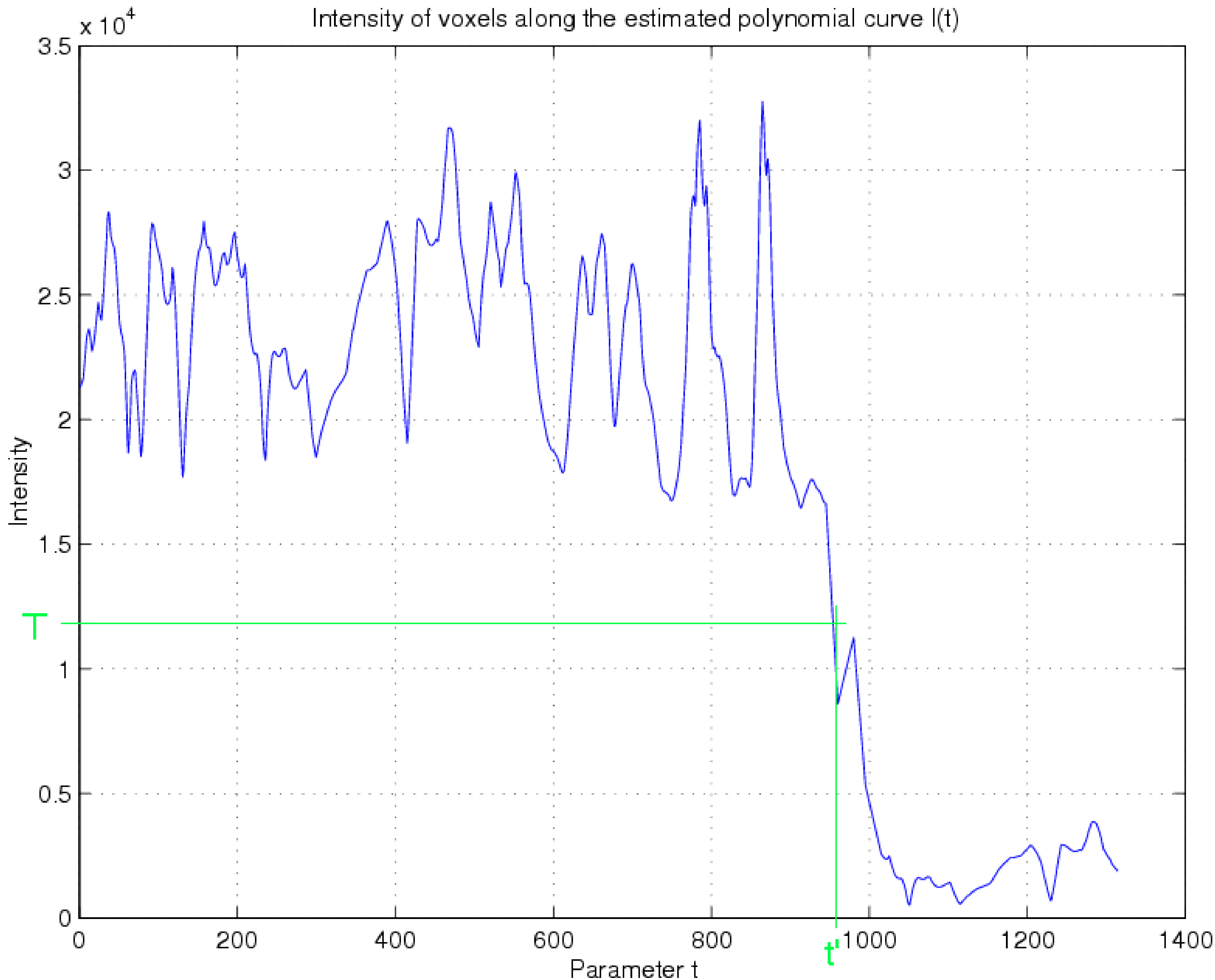
Intensity of voxels along the estimated polynomial curve I(t)
x 10^4
3.5
3
2.5
2
1.5
1
0.5
0
Intensity
T
0
200
400
600
800
1000
1200
1400
t'
Parameter t

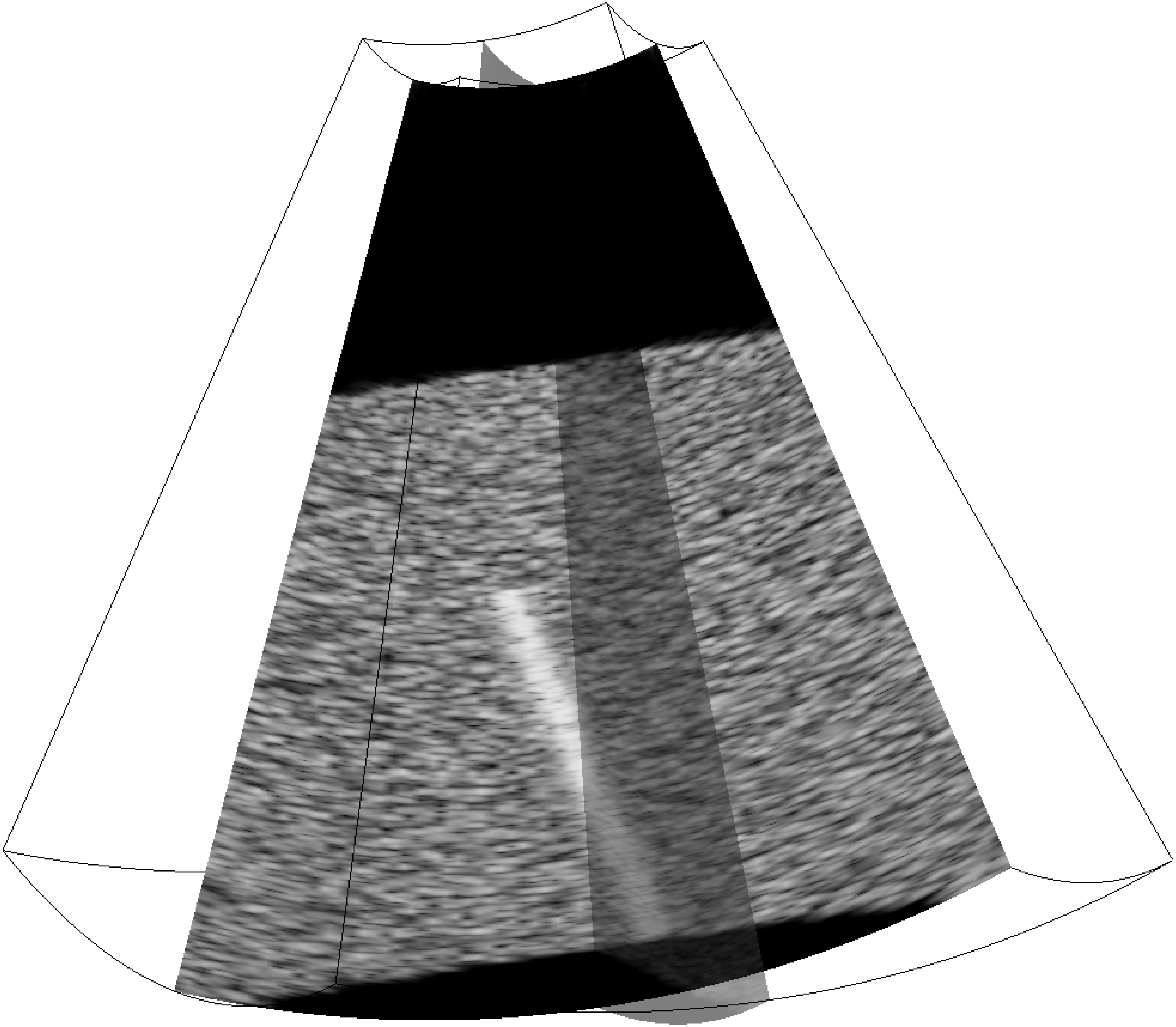

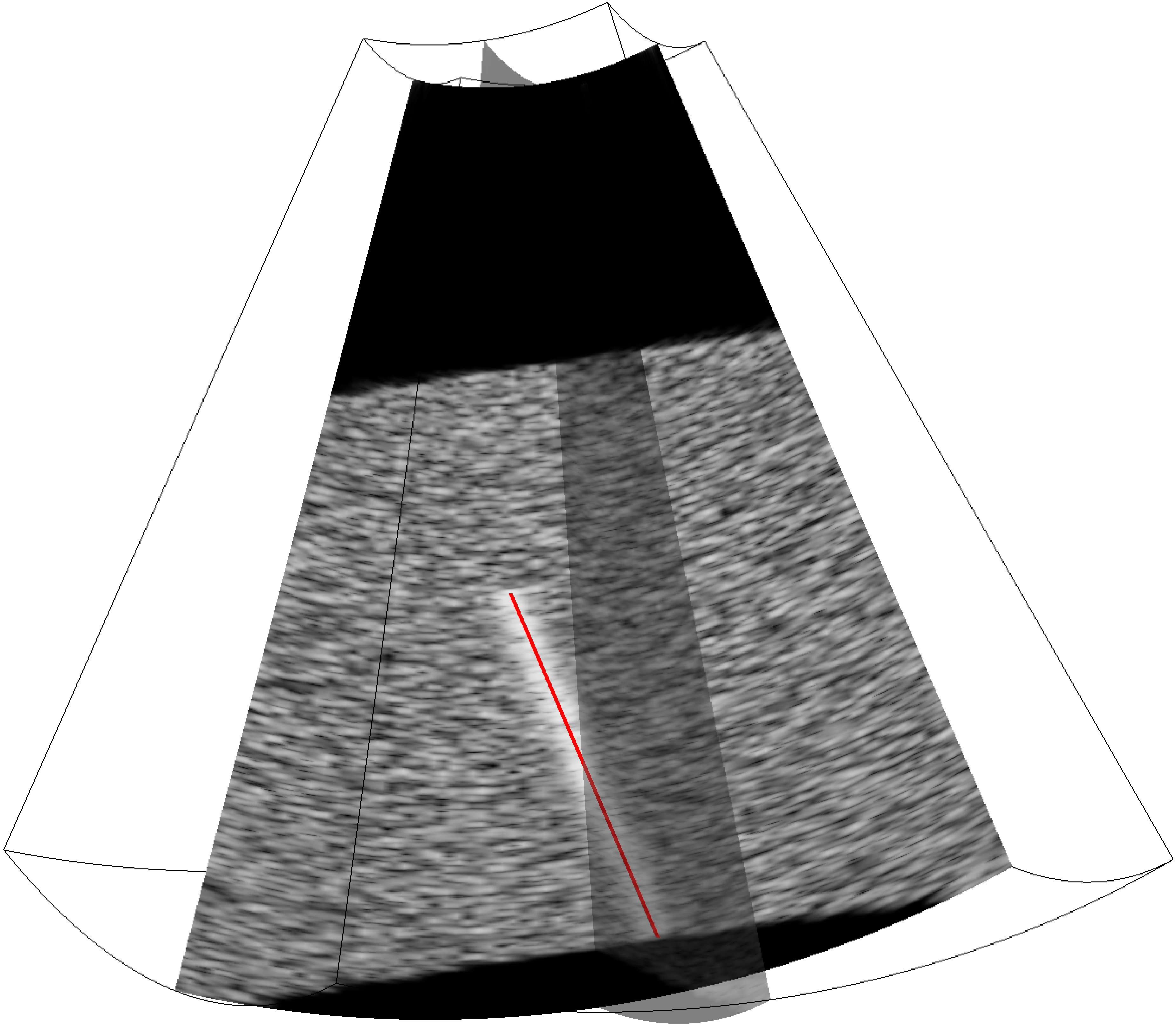

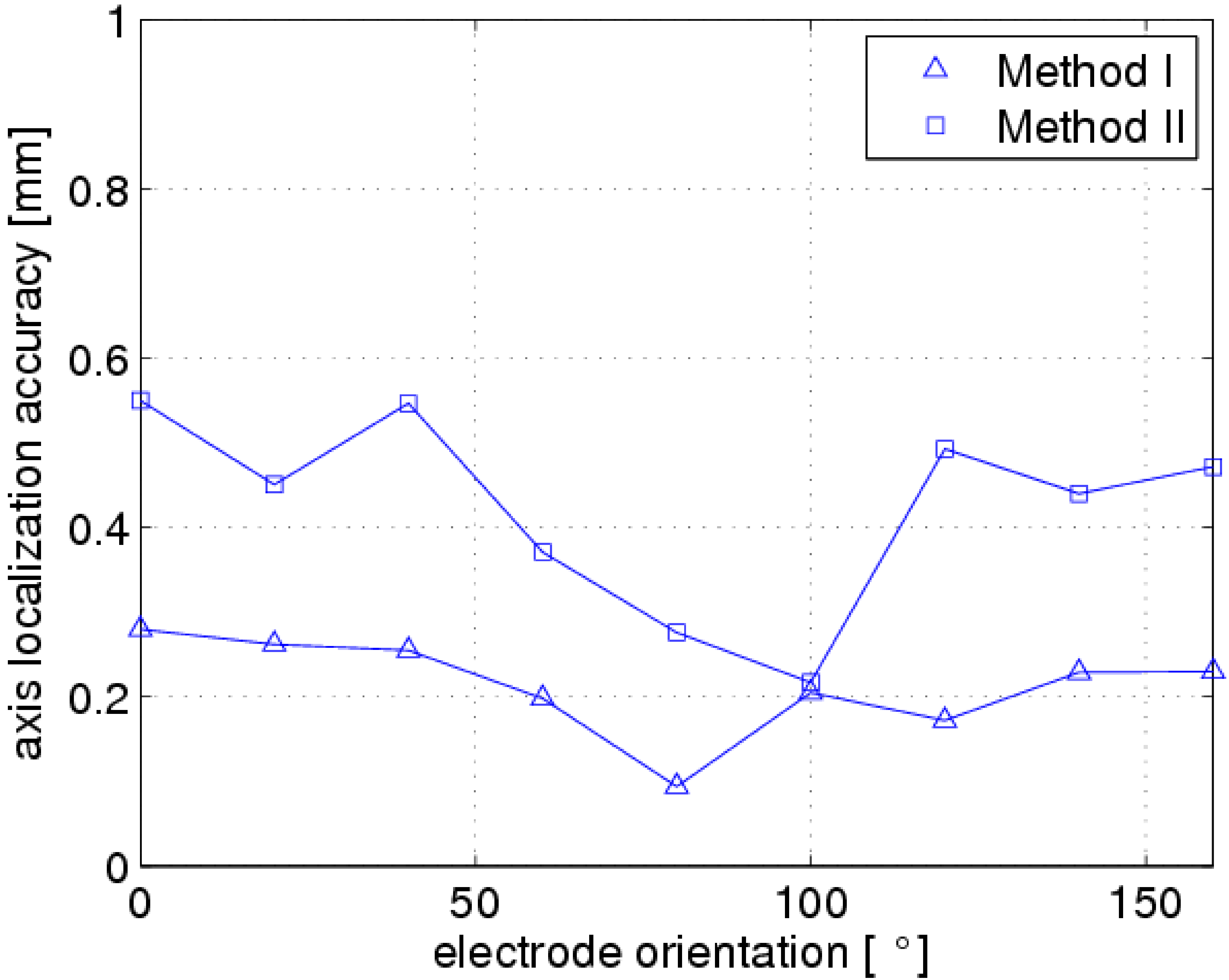
Method I
Method II
axis localization accuracy [mm]
electrode orientation [°]
0
0.2
0.4
0.6
0.8
1
0
50
100
150

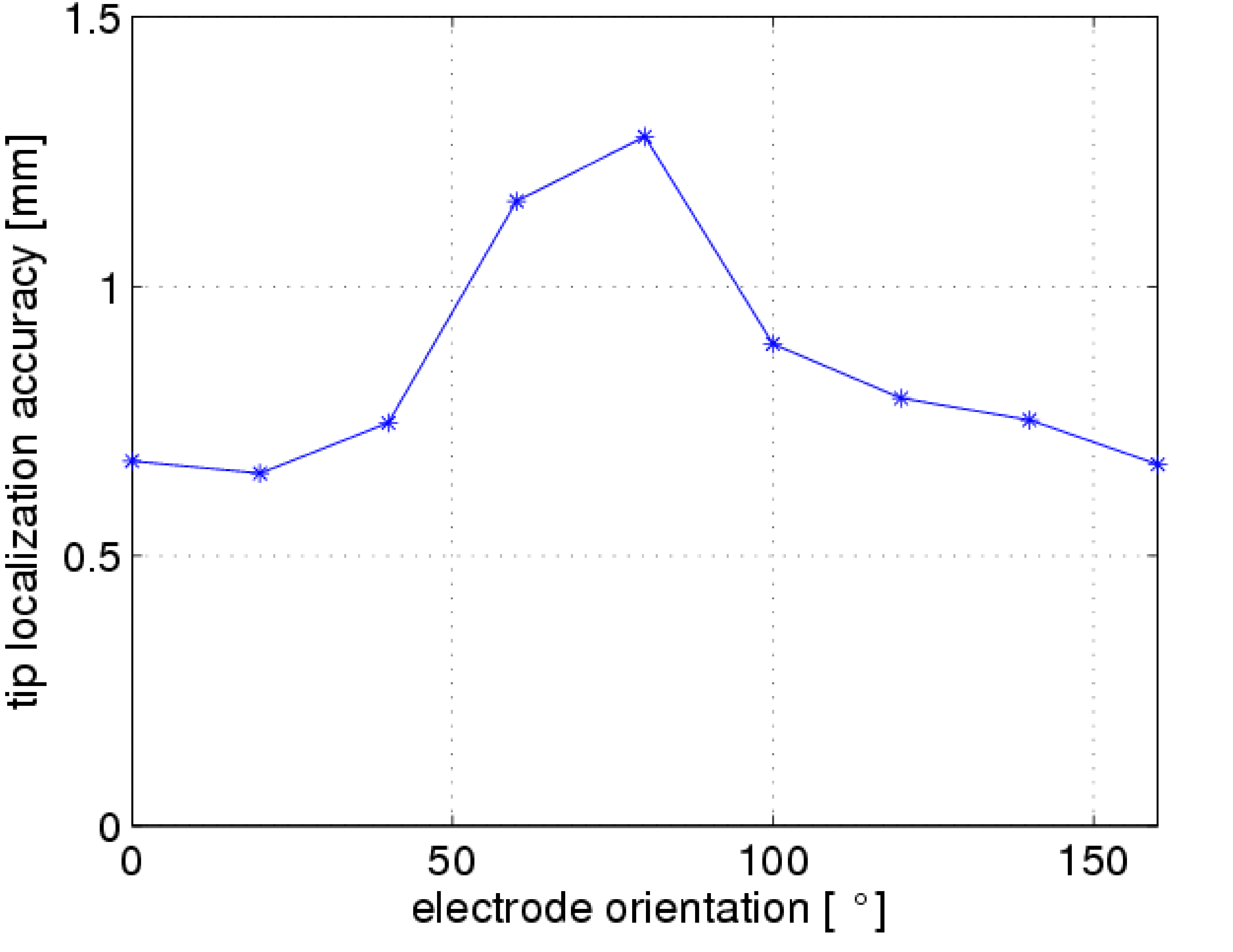

1.5
1
0.5
0
0
50
100
150
tip localization accuracy [mm]
electrode orientation [°]

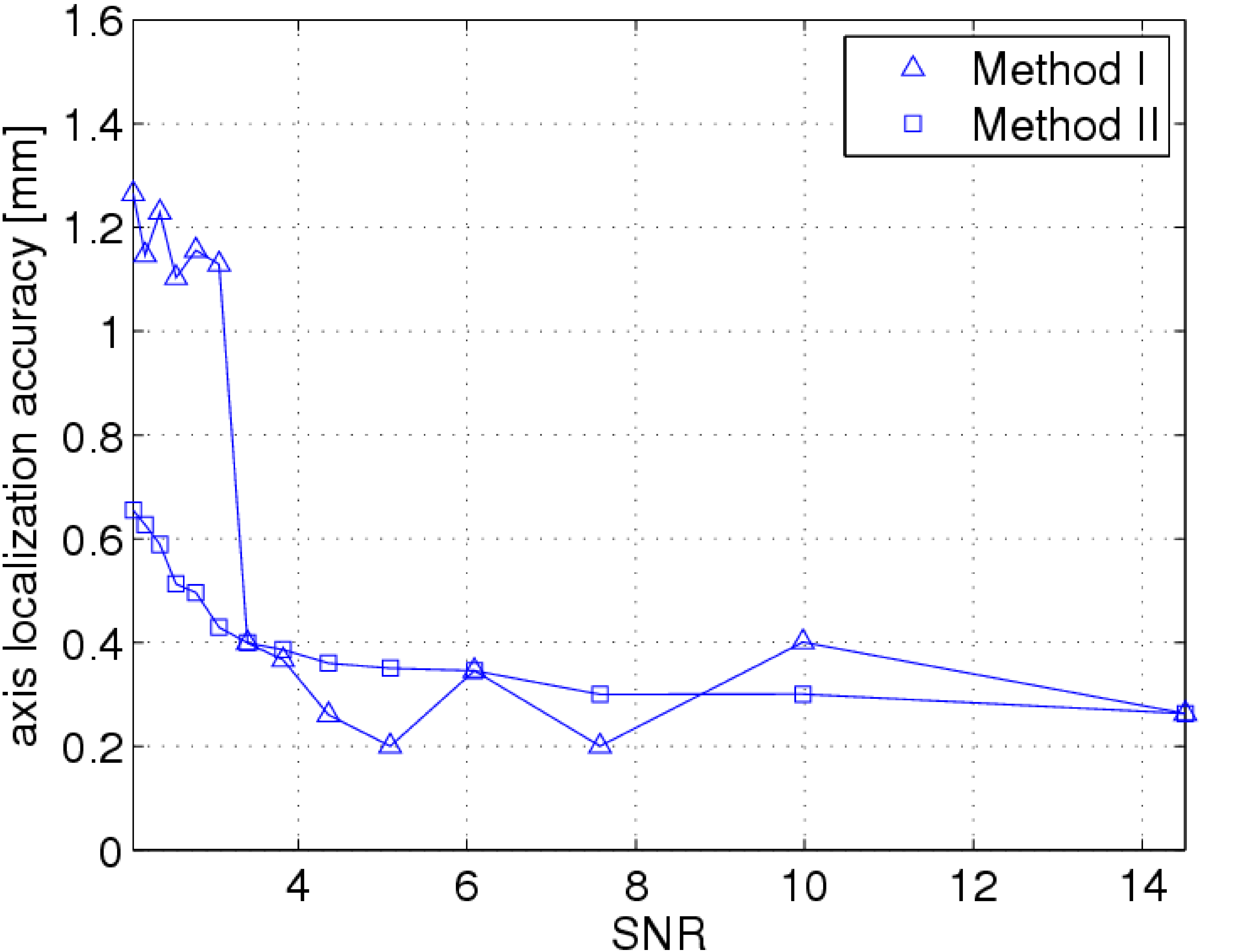

Method I
Method II
axis localization accuracy [mm]
SNR
0
0.2
0.4
0.6
0.8
1
1.2
1.4
1.6
4
6
8
10
12
14

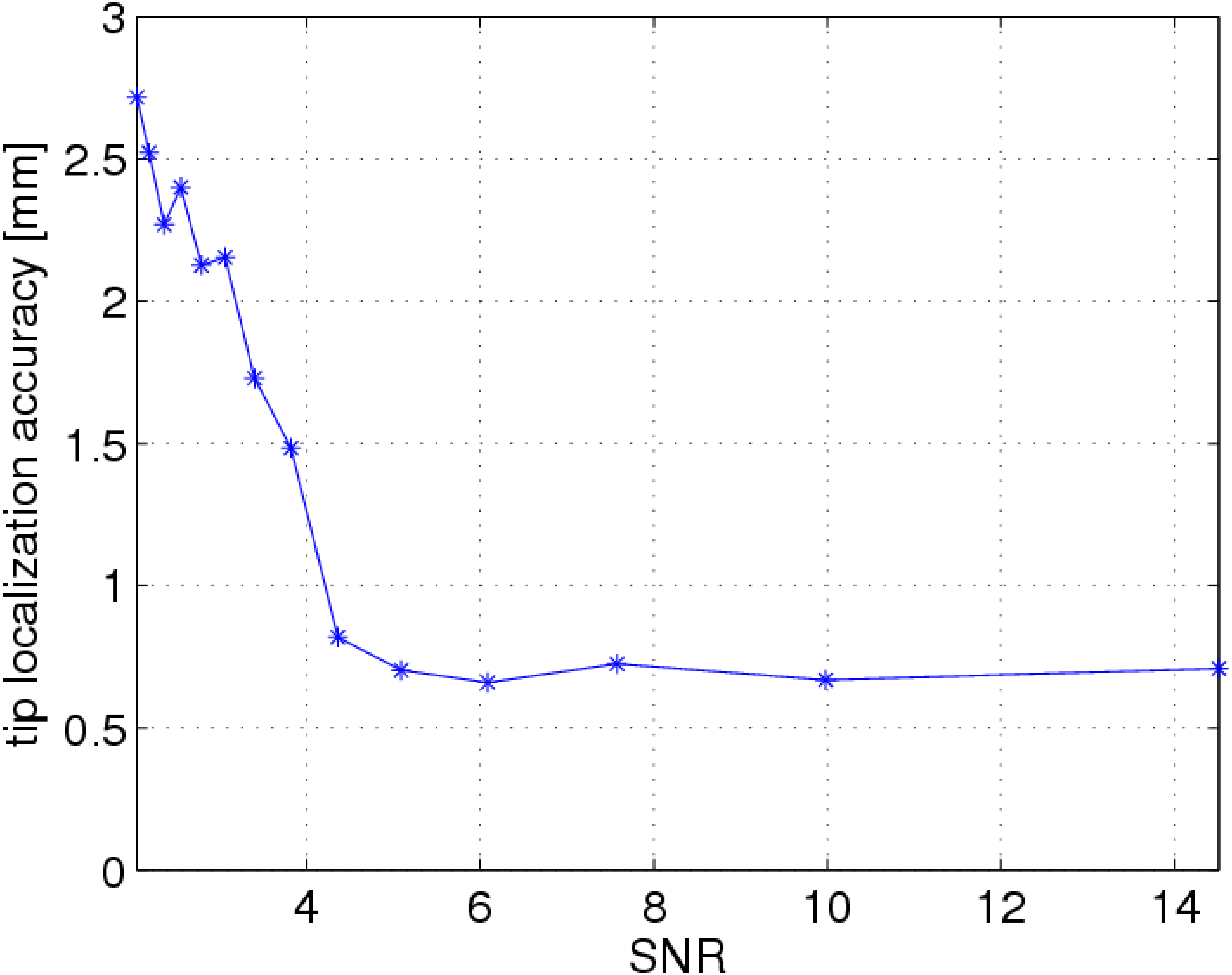

tip localization accuracy [mm]
3
2.5
2
1.5
1
0.5
0
4
6
8
10
12
14
SNR

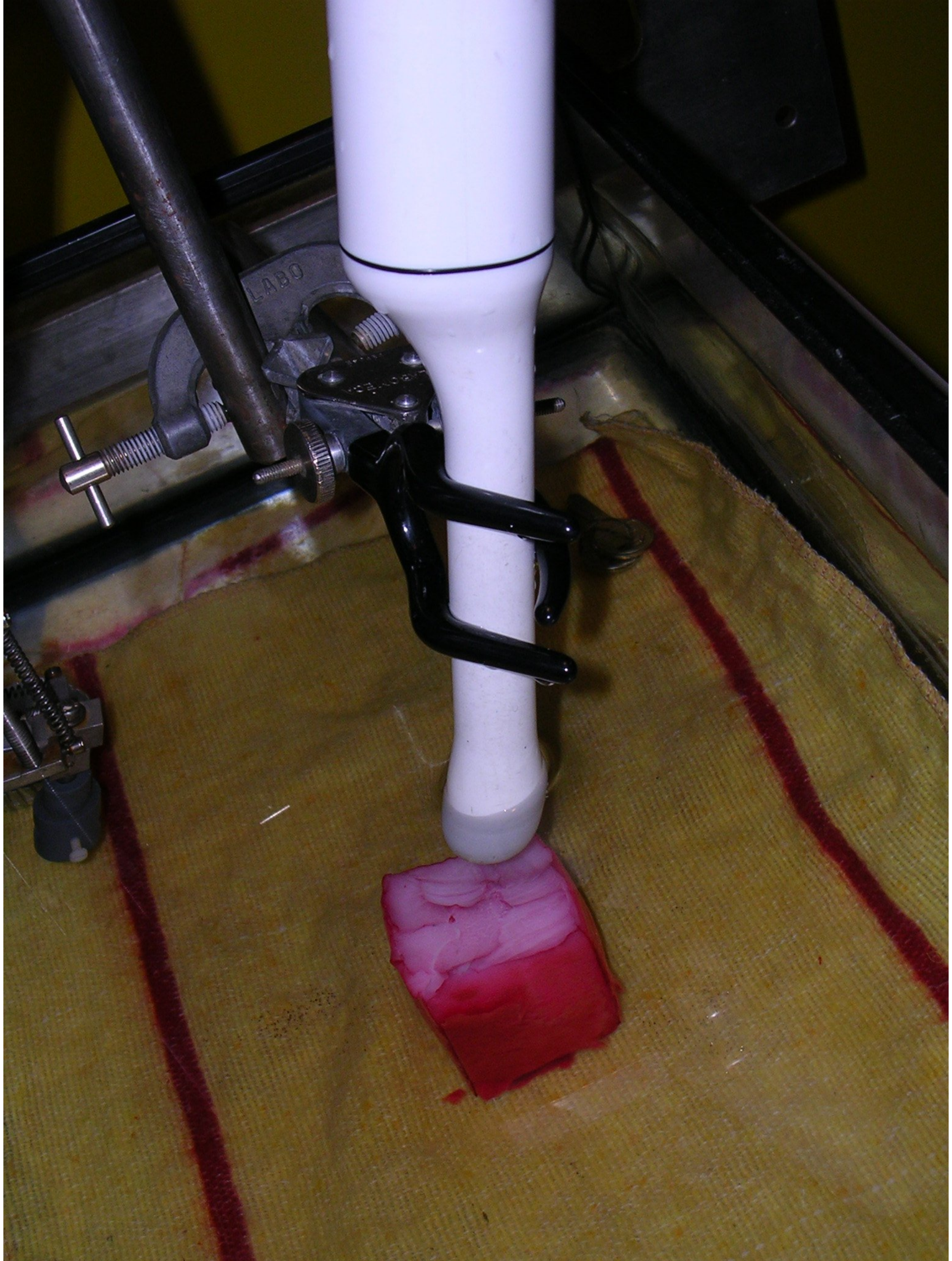

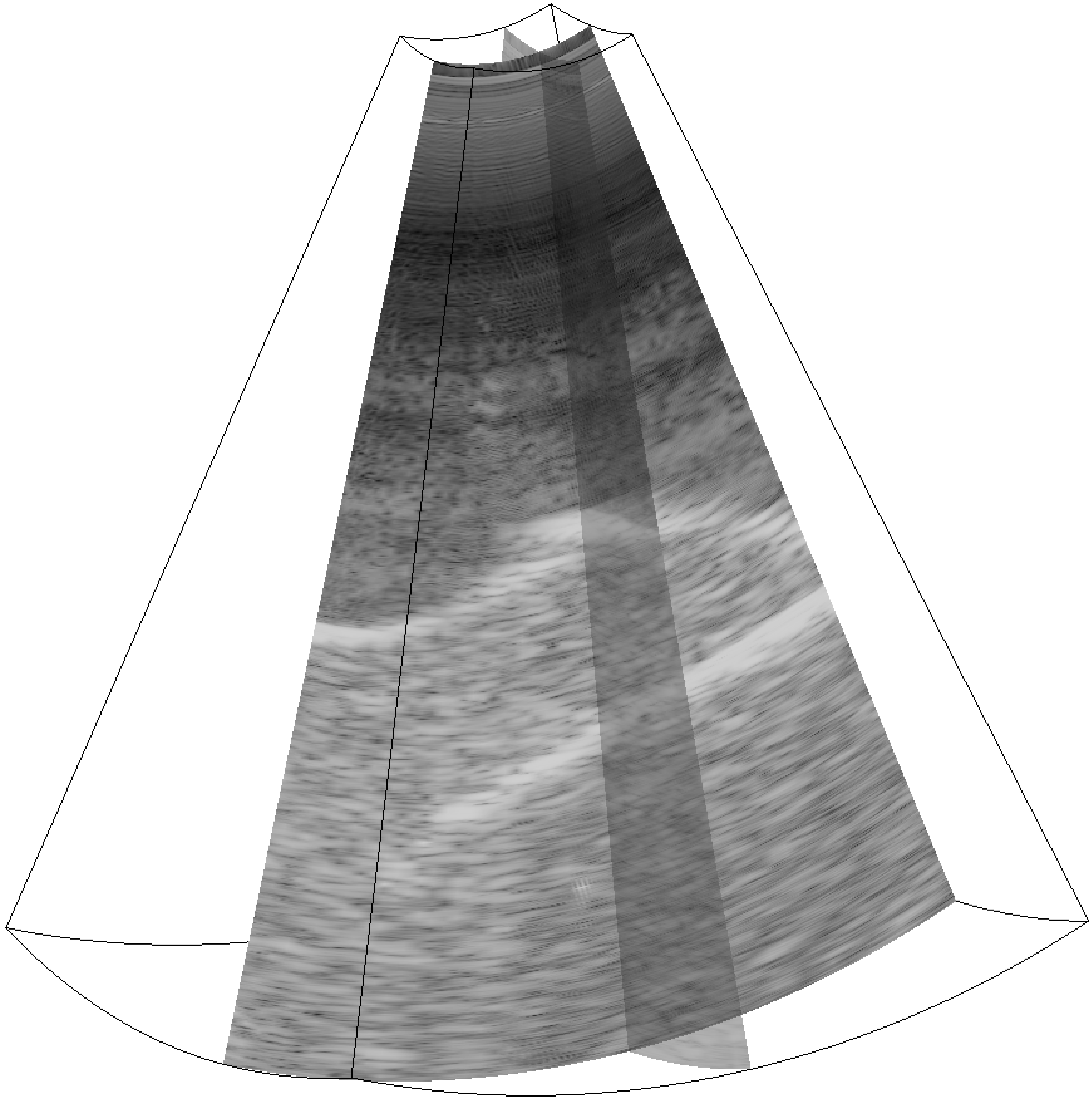

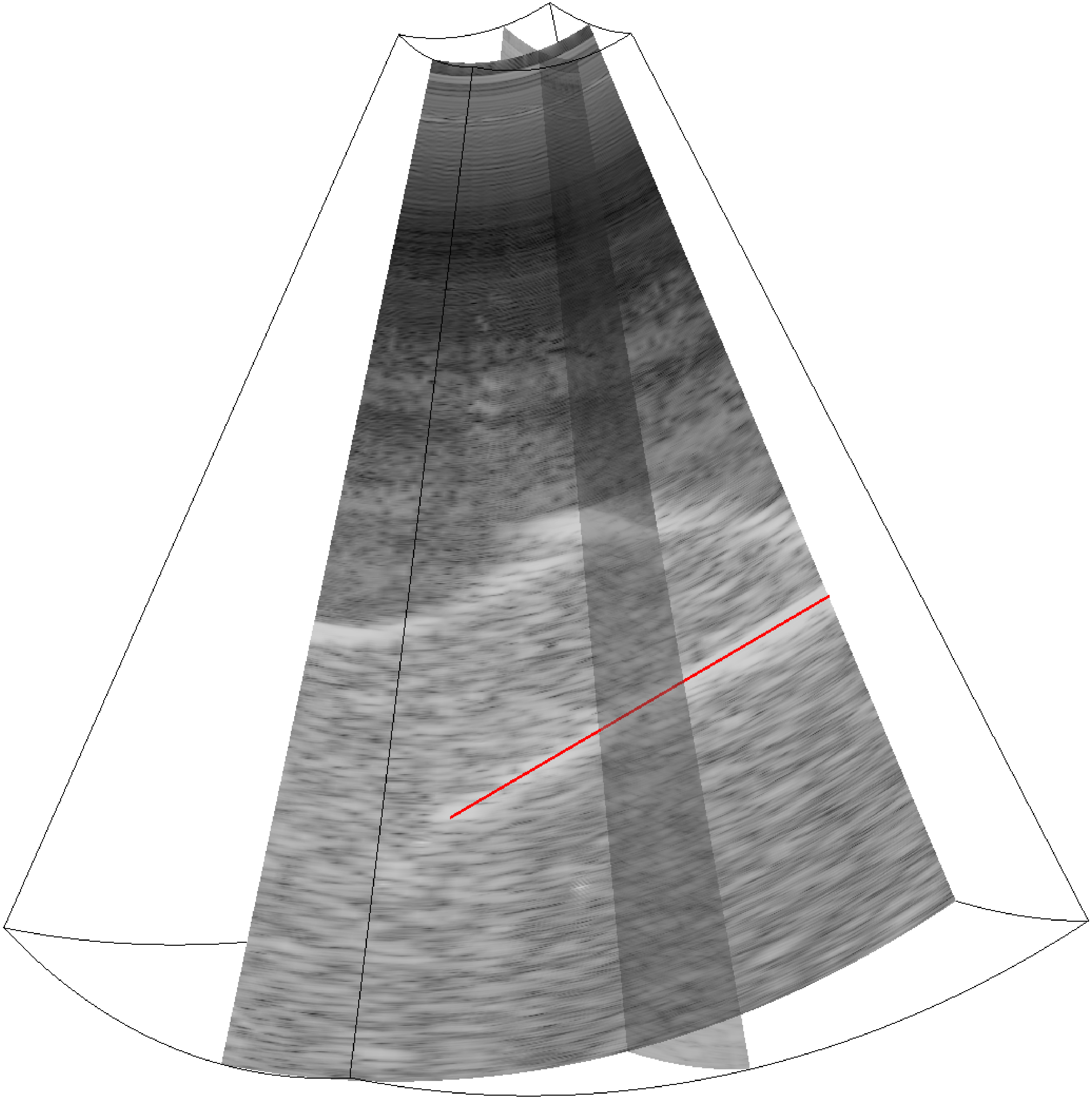

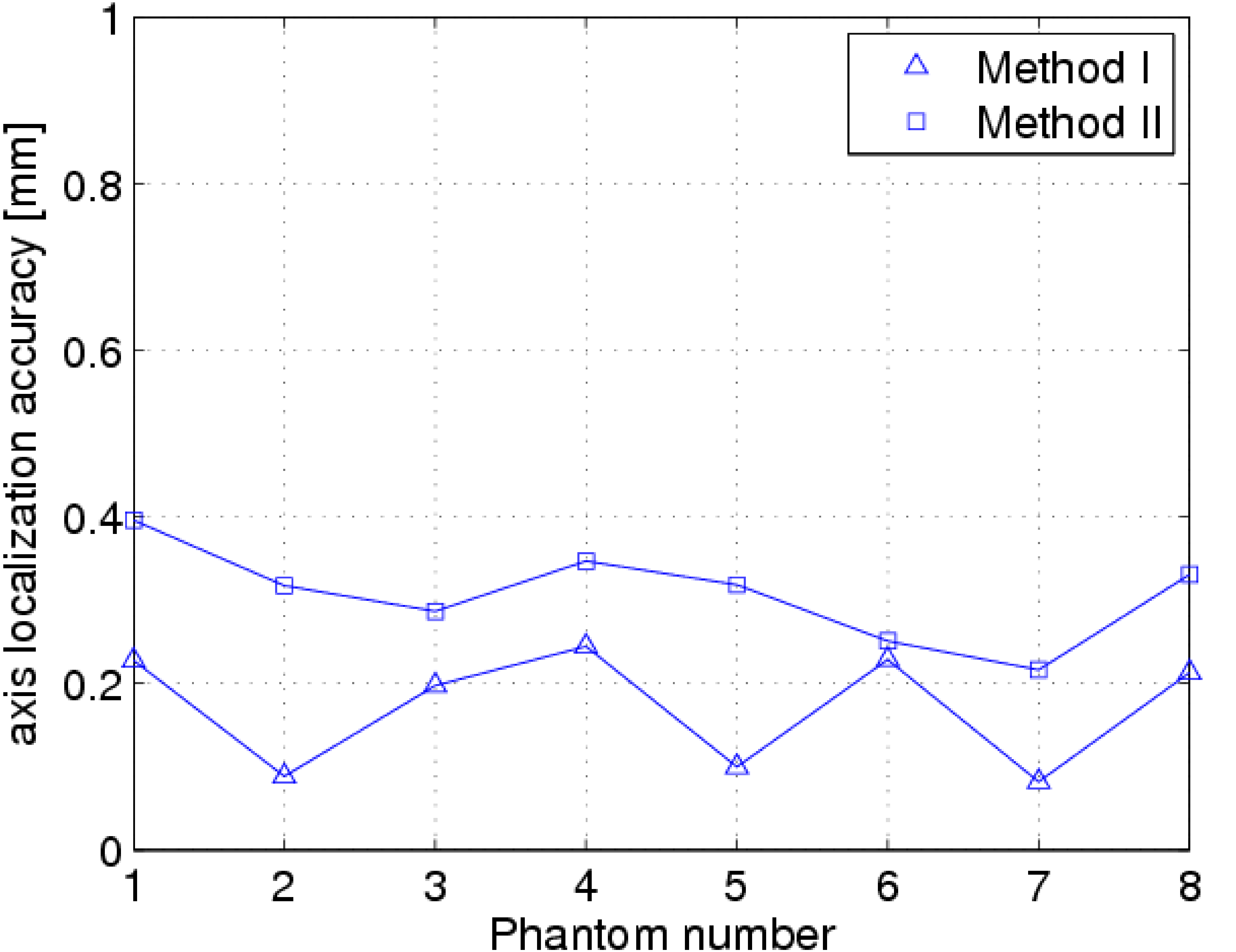

Method I
Method II
axis localization accuracy [mm]
Phantom number
0
0.2
0.4
0.6
0.8
1
1
2
3
4
5
6
7
8

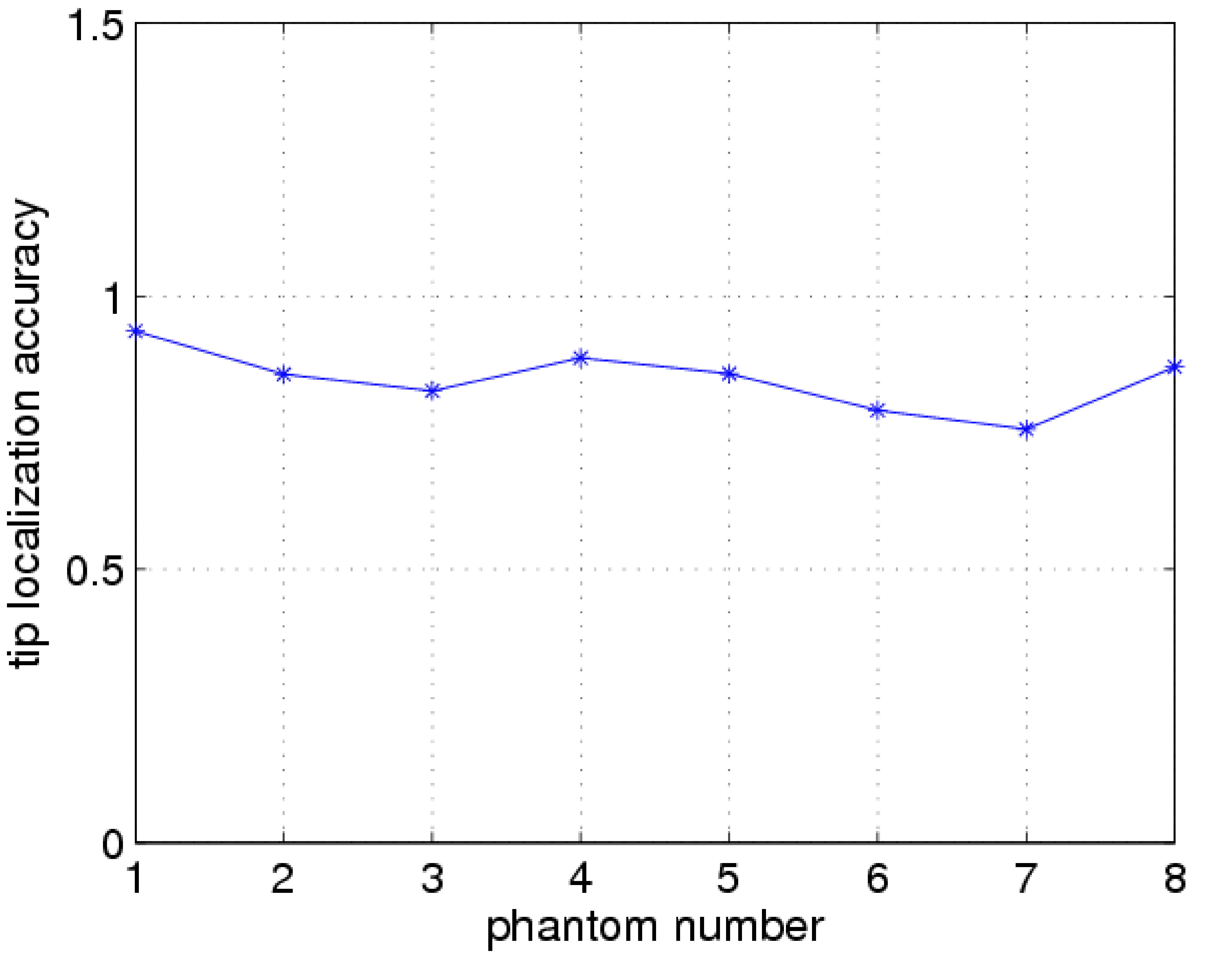

1.5
1
0.5
0
tip localization accuracy
1
2
3
4
5
6
7
8
phantom number


MERRY CHRISTMAS